Negative microfilm
received from university

66-6673

PARIZEK, Robert James, 1937-
THE MECHANISM OF THE NICKEL FERRITE FORMATION REACTION.

The University of Michigan, Ph.D., 1965
Engineering, metallurgy

University Microfilms, Inc., Ann Arbor, Michigan

THE MECHANISM OF THE NICKEL FERRITE FORMATION REACTION

Robert James Parizek

A dissertation submitted in partial fulfillment
of the requirements for the degree of
Doctor of Philosophy in the
University of Michigan
1965

Doctoral Committee:

Professor Maurice J. Sinnott, Chairman
Professor Dale M. Grimes
Professor Edward E. Hucke
Professor Guiseppe Parravano
Professor Lars Thomassen

To my wife, Jo Ann,

and my Parents

ACKNOWLEDGMENTS

The author wishes to express his appreciation to the members of his doctoral committee, Professors D. M. Grimes, E. E. Hucke, G. Parravano and L. Thomassen for their continued interest and advice. Special thanks are due to Professor M. J. Sinnott, chairman of the doctoral committee, for the assistance he so willingly provided during the experimental portion of the project, as well as during the writing of the dissertation.

The contribution of electron microprobe analyses by Mr. Frank Semer of the Ford Scientific Laboratories and Mr. Thomas H. West, Jr., of the General Atomic Division of The General Dymanics Corporation, and the nickel ferrites used as standards which were supplied by the Bell Telephone Laboratories, was much appreciated.

A National Science Foundation Graduate Fellowship enabled the author to concentrate his efforts on the academic requirements during his graduate study.

Finally, I feel deeply indebted to my parents for their advice and encouragement during the entire course of my education, and to my wife for the moral support she provided during the course of this work, as well as for typing the final copy of this dissertation.

TABLE OF CONTENTS

	Page
ACKNOWLEDGMENTS	iii
LIST OF TABLES	vi
LIST OF FIGURES	vii
ABSTRACT	ix
INTRODUCTION	1
LITERATURE SURVEY	3
Crystallographic Properties	4
Fe-Ni-O Phase Diagram	6
Chemical Reactions in the Solid State	10
Measurement of Extent of Reaction	11
Diffusion in Spinels	14
Experimental Results of Solid State Reaction Studies	17
Magnetic Properties	24
EXPERIMENTAL EQUIPMENT, PROCEDURES, AND MATERIALS	27
Experimental Equipment	27
Materials	29
Specimen Preparation, Treatment, and Analysis	31
RESULTS	36
ANALYSIS OF RESULTS	48
Cation Concentration Profiles	49
Formation of Ferrite Product	54
Magnetic Moment Measurement	58
Lattice Parameter Measurements	66
Optimum Conditions for Reaction	67
CONCLUSIONS	69
SUMMARY	71
APPENDICES	
A CALIBRATION OF ELECTRON MICROPROBE STANDARDS	73

TABLE OF CONTENTS CONT'D

		Page
B	MAGNETIC MOMENT OF NICKEL FERRITE.....	76
C	SPINEL REGION OF Fe-Ni-O PHASE DIAGRAM..	82
D	CALIBRATION OF FARADAY BALANCE.....	85
BIBLIOGRAPHY.....		86

LIST OF TABLES

Table		Page
I	Furnace Atmosphere Analyses.....	31
II	Interface Compositions in Diffusion Couples at 1200°C.....	50
A-I	Calibration of Electron Microprobe Standards	73
C-I	Spinel Field Boundary Compositions as a Function of Temperature and Atmosphere.....	82
C-II	Summary of Ferrite Compositions at Reactant-Product Interfaces in Nickel Ferrite System at 1200°C.....	84

LIST OF FIGURES

Figure		Page
1	Positions of Ions in Octahedral and Tetrahedral Sites. Arrangement of Sites in Ferrite Unit Cell.....	5
2	Ferrite Portion of Fe-Ni-O Ternary System Phase Diagram.....	8
3.	Schematic Isothermal Section of Ferrite Portion of Fe-Ni-O Phase Diagram at 1200°C...	9
4.	Magnetic Moment per Unit Mass Versus Reaction Time for Nickel Ferrite Formation in Different Atmospheres.....	18
5.	Magnetic Moment per Unit Mass Versus Reaction Time for 1:1 Mole Ratio NiO and Fe_2O_3 Samples in Different Atmospheres at 1200°C.....	38
6.	Magnetic Moment per Unit Mass Versus Reaction Time for 1:1 Mole Ratio NiO and Fe_2O_3 Samples in Different Atmospheres at 750°C.....	39
7.	Jander Plot of 750°C Reaction Rate Data on 1:1 Mole Ratio NiO and Fe_2O_3 Samples at 750°C	40
8.	Ginstling-Brounshtein Plot of 750°C Reaction Rate Data on 1:1 Mole Ratio NiO and Fe_2O_3 Samples at 750°C.....	41
9.	Magnetic Moment Versus Reaction Time for 1:1 Mole Ratio of NiO and Fe_2O_3.....	42
10.	Average Lattice Parameter Versus Reaction Time for Nickel Ferrite Fired in 1% O_2 at 1200°C.....	43
11.	Average Lattice Parameter Versus Reaction Time for Nickel Ferrite Fired in 21% O_2 at 1300°C.....	43
12.	Average Lattice Parameter Versus Reaction Time for Nickel Ferrite Fired in 21% O_2 at 1350°C.....	44
13.	Cation Concentration Profiles in NiO-Fe_2O_3 Diffusion Couple Reacted Four Days in 100% O_2 at 1200°C.....	45

LIST OF FIGURES CONT'D

Figure		Page
14.	Cation Concentration Profiles in NiO-Fe_2O_3 Diffusion Couple Reacted Four Days in 21% O_2 at 1200°C.....	46
15.	Cation Concentration Profiles in NiO-Fe_2O_3 Diffusion Couple Reacted Four Days in 1% O_2 at 1200°C.....	47
16.	Cation Concentration Profiles Across Product Reactant Interfaces. Ferrite Portion of Fe-Ni-O Phase Diagram.....	52
17.	Ferrite Portion of Fe-Ni-O Phase Diagram.....	54
A-1.	Comparison by X-Ray Diffractometer Peak Height of Bell Labs Samples with Specially Prepared Standards.....	74
A-2.	Comparison by Area Under X-Ray Diffractometer Peaks of Bell Labs Samples with Specially Prepared Standards.....	75
C-1.	Ferrite Compositions at NiO-Ferrite Interfaces and Fe_2O_3-Ferrite Interfaces as a Function of Furnace Atmosphere.....	83
D-1.	Calibration Curve for Faraday Balance.....	85

THE MECHANISM OF THE NICKEL FERRITE

FORMATION REACTION

by Robert James Parizek

ABSTRACT

Ferrite materials are formed in several different ways. One of the more common methods is to react mixtures of powdered oxides which will result in the desired product. These reactions are conducted at elevated temperatures and in furnaces in which the composition of the atmosphere can be controlled.

The study conducted was directed toward describing the reaction process during the formation of nickel ferrite from the component oxides, NiO and Fe_2O_3. Diffusion couple-type samples were prepared, fired under different oxygen partial pressures, and the resultant cation concentration profiles determined by the use of an electron microprobe. The corresponding oxygen contents were determined by relating the system to the ferrite region of the Fe-Ni-O phase diagram. In this manner the effect of variations in composition on the reaction process were predicted.

Magnetic moment measurements made on samples consisting of a one-to-one mole ratio of NiO and Fe_2O_3 powders intimately mixed, pressed into pellets, and fired in atmospheres of different oxygen contents for varying periods of time at 750°C and 1200°C indicated that the reaction rate

is controlled by the counter-diffusion of cations across the ferrite layer. These measurements also led to the conclusion that a decrease in the oxygen content of the furnace atmosphere increases the rate of formation of nickel ferrite.

It was found that the magnetic moment measurement as an indicator of extent of reaction can yield ambiguous results in systems of this type, in which the product formed is of non-uniform composition. If the proper precautions are observed, the results can be related mathematically to an assumed reaction model to ascertain the validity of that model in the situation under consideration. In this system, reaction temperatures of less than 1000°C yield a reaction product whose composition is uniform enough that the magnetic moment value is directly proportional to the amount of ferrite present.

It was determined that the optimum conditions for conducting this reaction are high reaction temperature (1500-1600°C) and high oxygen pressure (considerably in excess of one atmosphere). The high temperature is necessary to give a fast reaction. The high oxygen pressure reduces the composition variation in the product formed. Since the homogenization process is slow, it is desirable to form a uniform product and eliminate the necessity of long times for homogenization.

INTRODUCTION

Ferrite materials are formed in several different ways. One of the more common methods is to react mixtures of powdered oxides which will result in the desired product. These reactions are conducted at elevated temperatures and in furnaces in which the composition of the atmosphere can be controlled.

Preliminary experimental studies by the author showed that decreasing the oxygen partial pressure of the furnace atmosphere markedly increased the rate of formation of nickel ferrite from its component oxides, NiO and Fe_2O_3. A search of the literature revealed that this result has been reported by others, but that there was no reasonable explanation offered for this behavior. Consequently a more detailed experimental program was undertaken to describe the reaction process, and, thus, determine the causes of the observed effect.

Examination of the ferrite region of the Fe-Ni-O phase diagram indicated that the cation concentration gradients within the ferrite product during the reaction should be dependent on the oxygen content of the atmosphere. It was anticipated that these gradients would alter the reaction rate in the manner observed. Thus the experimental program was directed toward evaluating this effect on the reaction.

During the course of the work it was necessary to evaluate other factors which are an inherent part of the

system. The effect on the reaction rate of variations in cation diffusivities as related to variations in ferrite composition was considered. An examination of the variations in composition as related to the magnetic moment as a means of measuring the progress of reactions of this type was also conducted. The description of the reaction process developed during the course of the study enabled the optimum conditions for the conduct of the reaction to be predicted.

LITERATURE SURVEY

The items covered in this Literature Survey are those concerned with either the experimental work performed or the phenomenological description of the reaction under consideration. The crystallographic properties of the spinels in general, as well as nickel ferrite specifically, are described briefly. The discussion of the phase diagram is restricted to the ferrite region of the Fe-Ni-O system. The effects of variations in temperature and oxygen partial pressure are covered, along with the relationship of the excess oxygen in the ferrite to the cation vacancy concentration.

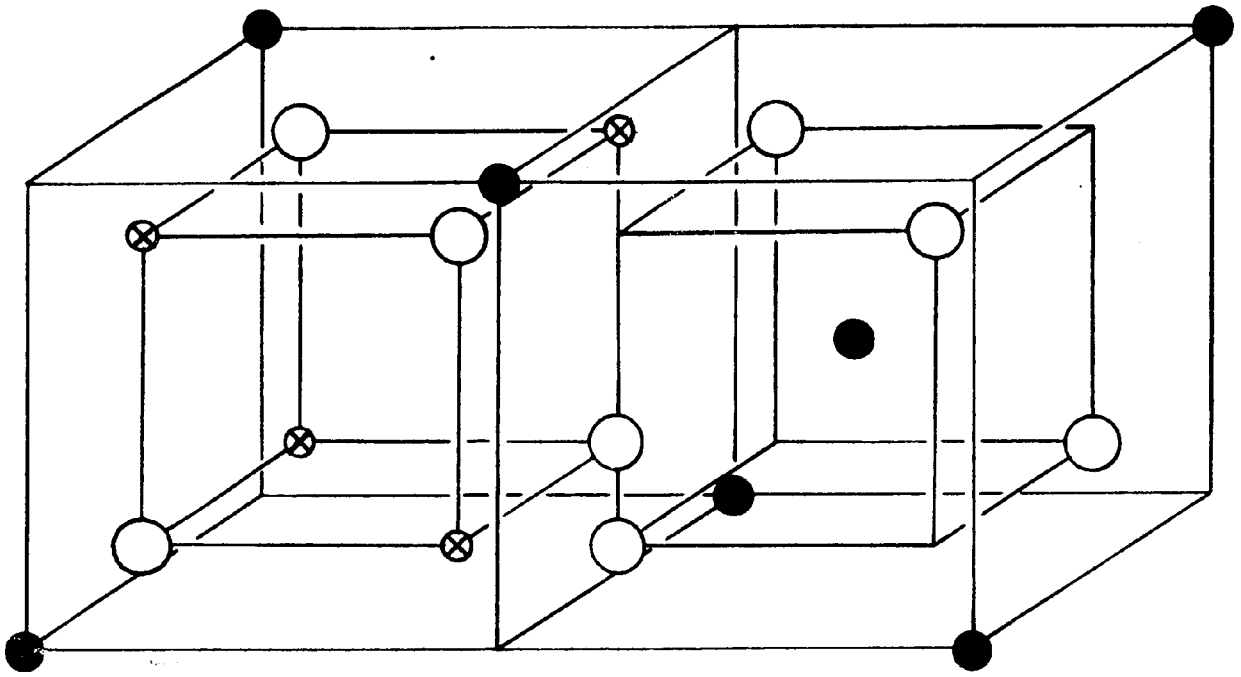
A general description of solid state chemical reactions leads to the mechanism proposed by Wagner (1, 2) for solid state reactions. Several methods of relating the amount of product formed to the reaction time are discussed, followed by comments on magnetic moment as a measure of the amount of product formed.

The effect of composition changes and cation vacancy concentration on cation diffusivities is discussed, followed by a description of some of the published experimental results and theories concerning spinel formation reactions. Finally, some of the variables affecting magnetic properties are discussed.

Crystallographic Properties

The crystallographic class of materials known as spinels all have the same crystal structure as the natural mineral spinel, $MgAl_2O_4$. The general structure of the spinels consists of a unit cell containing eight molecules of $Me^{+2}Me_2^{+3}O_4$, where Me^{+2} designates a divalent cation and Me^{+3} designates a trivalent cation. Thus the unit cell contains 32 oxygen ions, which are arranged in a cubic close-packed array. This arrangement of oxygen ions leads to two different types of sites in the oxygen lattice into which the cations may be placed: tetrahedral (A) sites, which have four oxygen ions as nearest neighbors, and octahedral (B) sites, which have six oxygen ions as nearest neighbors. Within the oxygen lattice of the unit cell, there are 96 of these cation sites, of which 64 are of the tetrahedral and 32 are of the octahedral type. Of these available sites, it is found that eight of the 64 tetrahedral sites and 16 of the 32 octahedral sites are occupied in the stoichiometric spinel. Figure 1 shows the positions of the ions in both types of sites, and the arrangement of the sites in the unit cell.

Spinels can be classified according to the distribution of cations in the different types of lattice sites. Those which have the divalent cations on the tetrahedral sites and trivalent cations on the octahedral sites are known as normal spinels, while those which have the eight divalent ions on the octahedral sites and the sixteen trivalent ions

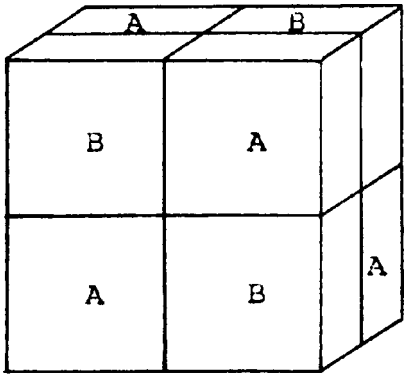


Octahedral (A) Sites Tetrahedral (B) Sites

⊗ - Octahedral Site

● - Tetrahedral Site

○ - Oxygen Ion



$Me_8Fe_{16}O_{32}$

Spinel Unit Cell

Figure 1. Positions of Ions in Octahedral and Tetrahedral Sites. Arrangement of Sites in Ferrite Unit Cell.

distributed on the eight tetrahedral sites and eight remaining octahedral sites are known as inverse spinels. Those which have a cation distribution somewhere between these extremes are known as intermediate spinels.

Nickel ferrite, $NiFe_2O_4$, is representative of the inverse type of spinels. Skolnick, Kondo, and Lavine (3) used an x-ray method to establish the cation distribution of nickel ferrite experimentally. Their results showed that $\emptyset$, the fraction of ferric ions displaced from the octahedral sites, was 0.483 ± 0.020. (A value of $\emptyset = 0.5$ indicates the completely inverse type.)

Shafer (4) has shown that the lattice parameter of nickel ferrite varies continuously, and in accordance with Vegard's Law, from 8.3885 Å for Fe_3O_4 to 8.3394 Å for $NiFe_2O_4$. Gluck (5) has written a digital computer program for determination of lattice parameters in cubic materials which can be applied to ferrites. Special features incorporated in his program are that the Nelson-Riley extrapolation technique is used with a least-squares fit of the data employed in the extrapolation. Diffraction angles of less than 30° are disregarded, and, in the back reflection region, the α_1 and α_2 doublets are utilized where they are resolved. An estimate of the standard deviation of the parameter is also made.

Fe-Ni-O Phase Diagram

This discussion of the ternary phase diagram for the Fe-Ni-O system is based on the work of Darken and Gurry (6)

on the Fe-O system, and that of Paladino (7) and Shafer (8) for the Fe-Ni-O system from 1000°C to 1300°C and from 1400°C to the liquid region respectively.

Figure 2 shows that portion of the three dimensional representation of the ternary system which is of interest to this discussion. The right face of the diagram is taken from the Fe-O system, while the rest of the diagram represents features within the ternary region of the system.

It should be noted that the solid solution of oxygen in Fe_3O_4, designated Fe_3O_4(SS), is extended into the ternary diagram as the nickel content is increased. This solubility region decreases in width as the nickel content is increased, until, at the line designated $NiFe_2O_4$, the region has zero width. It should also be noted that as temperature decreases, the width of the solid solution region decreases for any given nickel content.

The dashed lines in Figure 2 indicate the relative positions of an oxygen isobar at different temperatures in the system. Figure 3, part of a schematic isothermal section of this system at 1200°C, shows the paths of different oxygen isobars.

The existence of a (Ni, Fe)O solid solution has been shown by several investigators (9, 10). It is this solid solution, rather than pure NiO, which is actually in equilibrium with nickel ferrite in this system. On the other hand no significant amount of solid solution of nickel in Fe_2O_3 has been reported.

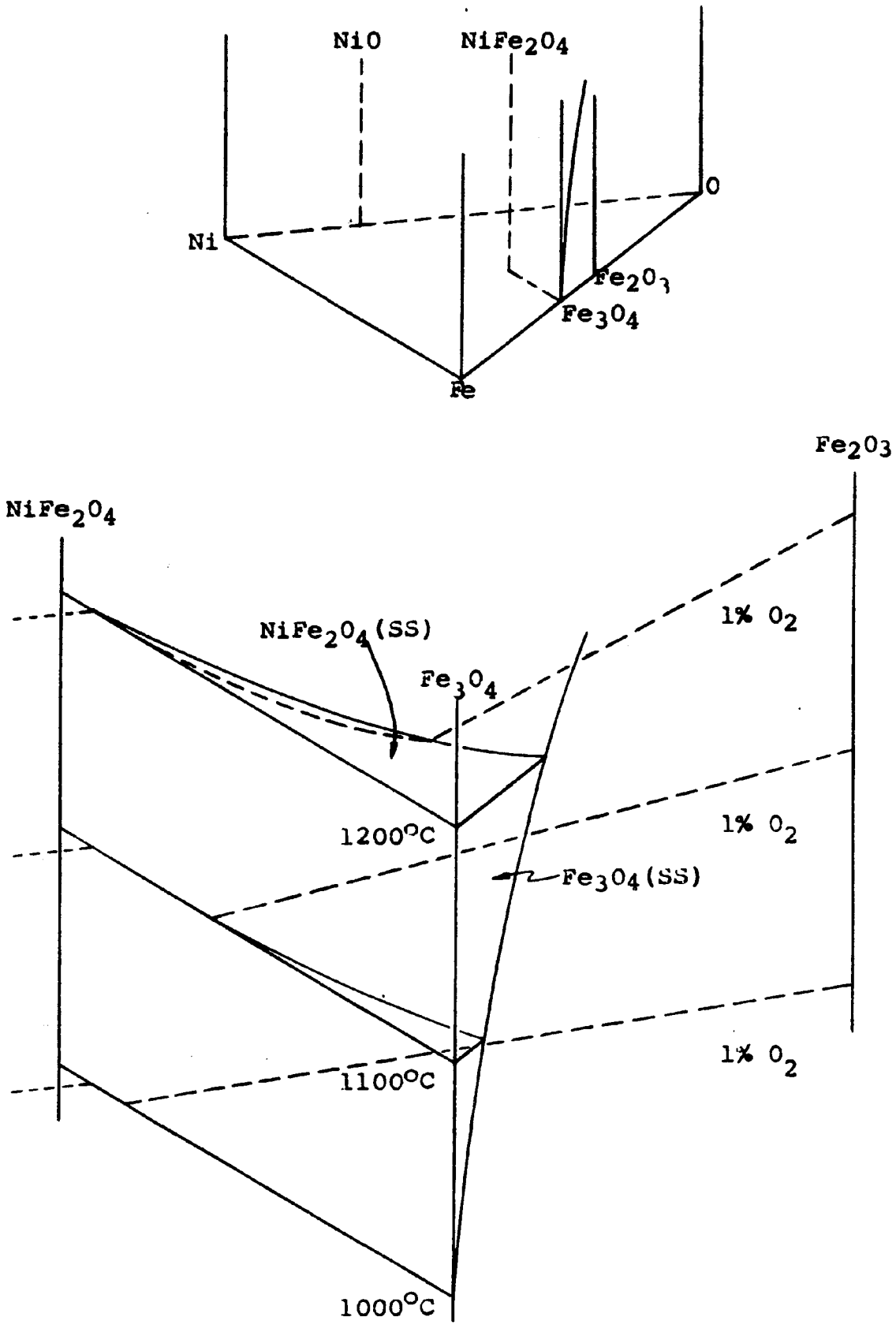


Figure 2. Ferrite Portion of Fe-Ni-O Ternary System Phase Diagram

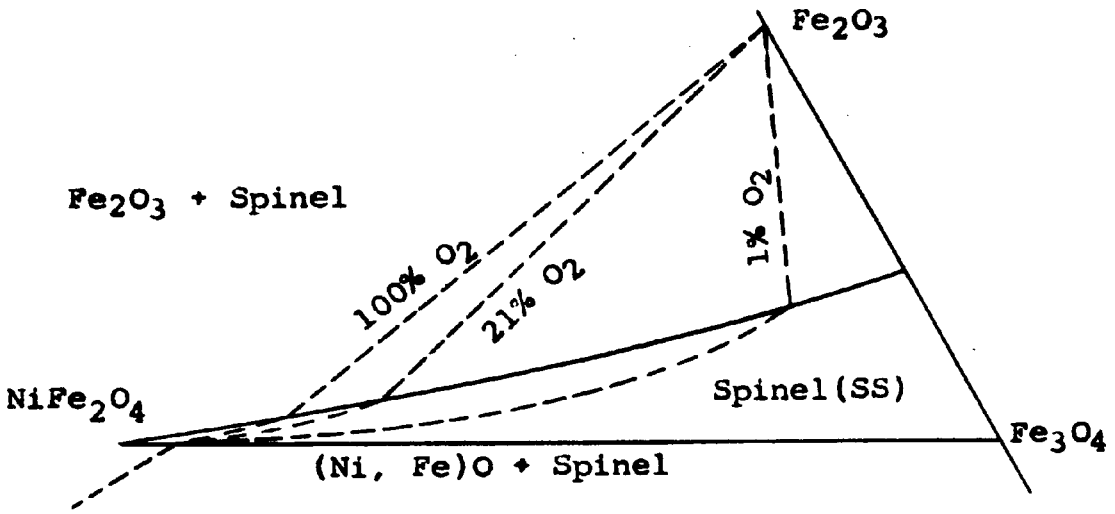


Figure 3. Schematic Isothermal Section of Ferrite Portion of Fe-Ni-O Phase Diagram at 1200°C.

The straight line connecting the points designated $NiFe_2O_4$ and Fe_3O_4 represents those compositions having a ratio of three cations to four anions, a composition referred to hereafter as stoichiometric. The use of the formula, $NiFe_2O_4$, is restricted to the material which has a ratio of three cations to four anions and an Fe:Ni ratio of 2.0. The term nickel ferrite is used when referring to ferrite of any other composition.

A material whose composition is represented by a point within the solid solution region is said to contain excess oxygen. However, it has been shown (11, 12) that ferrites containing excess oxygen actually develop cation vacancies, rather than accepting the oxygen interstitially. Thus the terms "excess oxygen" and "cation vacancies" are often used interchangeably.

In a more recent study, Shafer (4) has determined that

nickel ferrite containing excess nickel can be formed, but this occurs only at oxygen pressures in excess of one atmosphere. He was also able to establish that the ferrite was formed by replacing Fe^{+3} on the octahedral sites by Ni^{+3}.

Chemical Reactions in the Solid State

According to Jefferson (13) true solid state reactions proceed under a driving force which is the chemical potential gradient in the specimen. This gradient of chemical potential leads to diffusion of the ions to positions in which they react with the other ions.

The kinetics of solid state reactions are generally governed by one of two steps in the reactions: the rate of reaction at the reaction interface, or the rate of diffusion of the reacting components to this interface. When expressed in mathematical form, we have:

$$\frac{dy}{dt} = \frac{k}{y + b}$$

where y = product layer thickness

t = time

k, b = constants.

This expression includes both of the governing steps, as can be seen in the limits of the expression. For small values of y, i.e., very little reaction product formed, the expression is approximately dy/dt = k/b, which, upon integration, becomes y = k't. For large y, indicating a large amount of product formed, the original expression

becomes $dy/dt = k/y$, which, when integrated, becomes $y^2 = k''t$, an expression which is known as the parabolic law, and which is true for diffusion-controlled processes.

The movement of ions in solid materials has been discussed by Wagner (1, 2). He interprets the facts of the formation of compounds in the solid state in the light of his theory of ion movement in these materials. The formation of spinels is interpreted as resulting from the diffusion of the cations of the component materials in an internal electrical field, due to the ionic charges present, to a reaction interface, while the anions form the matrix through which the cations diffuse.

For the case of nickel ferrite formation, the Wagner hypothesis leads to the following reaction scheme:

NiO	$NiFe_2O_4$	Fe_2O_4

Ion Diffusion $3Ni^{+2} \longrightarrow$ $\longleftarrow 2Fe^{+3}$

Phase	$4NiO$	$4Fe_2O_3$
Boundary	$-3Ni^{+2}$	$-2Fe^{+3}$
Reactions	$+2Fe^{+3}$	$+3Ni^{+2}$
	$NiFe_2O_4$	$3NiFe_2O_4$

Measurement of Extent of Reaction

Since reaction rates are generally based on volumetric

measurements, expressions have been developed which relate the reaction rate and the volume of the product formed. The original expression, due to Jander (14), is:

$$\left(1 - \sqrt[3]{\frac{100 - x}{100}}\right)^2 = \frac{2\,kt}{r^2} = k't$$

where x = volume percent reacted

k, k' = constants

t = reaction time

r = radius of particles.

This expression is based on two assumptions which lead to significant deviations from reality at large conversions: first, the analysis is based on a combination of planar and spherical particle shapes, while the boundary conditions are based on spherical particles; and, second, it is assumed that the specific volumes of reactants and products are equal. Both of these assumptions are sufficiently good at low conversions, but result in deviations at higher conversions.

Carter (15) has formulated an expression which eliminates these difficulties and, thus, gives more accurate results at high percentages of conversion. His expression, based on spherical particles reacting with a gas, is:

$$\left[1 - (z - 1)x\right]^{2/3} + (z - 1)(1 - x)^{2/3} = z + \frac{2(1 - z)kt}{r^2}$$

where x = fraction reacted

z = volume ratio, products to reactants

k = constant

t = reaction time

r = particle radius.

Carter followed the oxidation of uniformly sized nickel spheres and was able to experimentally verify this expression.

Ginstling and Brounshtein (16) have derived essentially the same equation as Carter, but they neglected the effect of the volume change. Their expression is:

$$\frac{2}{3}x + (1 - x)^{2/3} = 1 - \left(\frac{k}{r^2}\right)t$$

where x = fraction reacted

k = constant

r = particle radius

t = reaction time.

Carter (17) concludes that the equation of Ginstling and Brounshtein is valid for $z \leq 2$, so that most kinetic data can be analyzed adequately using the simpler expression of Ginstling and Brounshtein. He also states that only rarely are the boundary conditions, on which the equations are based, met in strict sense. Thus, he concludes that to determine if a solid state reaction is diffusion controlled, to find its activation energy, or to determine the relative reactivities of powders, it is not necessary to have uniform or spherical particles, but only to have identical samples, and constancy of reacting area. The desired information can then be derived from a plot of x^2 versus t (square of fraction reacted versus time). This assumes that the reacting particles

are planes of infinite extent, and is generally valid until x reaches 0.6 or 0.8.

The measurement of the extent of reaction in ferrite materials generally depends on the magnetic properties of the substances. The component oxides MeO and Fe_2O_3 are anti-ferromagnetic, while the ferrite formed by the combination of these oxides is ferrimagnetic. Thus the measurement of the magnetic moment of a sample gives a measure of the amount of ferrite present, and subsequently a measure of the amount of transformation of the oxides into the ferrite. Turnbull (18) states that it is unlikely that a second magnetic component could contribute to the apparent magnetic moment of samples of nickel ferrite, noting that "γ - Fe_2O_3 is relatively unstable at temperatures above 400°C, and also that no evidence for this component was found by x-ray analysis" in his work. Since this measure of magnetic moment is a volume property of the material, it seems ideally suited to analysis by the methods outlined in this section.

Diffusion in Spinels

Lindner (19) has observed that the self-diffusion of cations is usually higher in spinels than in pure oxides, although the activation energies in both cases are comparable. Thus, he justifies the assumption of a Wagner-type mechanism for spinel formation. He also notes that an increase of the concentration of the iron (probably as Fe^{+3}) of 3-5% in zinc ferrite ($ZnFe_2O_4$) increases the diffusion coefficient of iron by about a factor of ten, but does not affect the self-diffusion coefficient of zinc.

Birchenall (20), in discussing the growth of spinels during oxidation, concludes that the work of Lindner (21) and others (22, 23, 24) shows that cation mobilities in spinels are greatly affected by composition. The case of magnetite (25) is interesting, because the cation mobility seems to be greater than in any other spinel. Diffusion of octahedral cations must occur via a tetrahedral site, and vice versa. Although it is not known which of these procedures contributes more to the iron ion mobility, Verwey and Haayman (12) have suggested that excess oxygen in the structure results in cation vacancies on the octahedral sites in preference to the tetrahedral sites. The high electron mobility of magnetite, as evidenced by the high conductivity, along with the presence of both Fe^{+2} and Fe^{+3} on the octahedral sites, implies that it is very easy to provide either Fe^{+2} or Fe^{+3} at any specific site. Thus, if one form, perhaps the smaller Fe^{+3}, is more favorable for diffusion, the fact that this form can be easily provided means that diffusion can occur readily. Romeijn (26) has shown that Fe^{+3} has no preference for one type of site over the other due to crystal field splitting of the electron energy levels, but McClure (27) has shown that Fe^{+2} has a preference for octahedral sites amounting to about 3.9 kilocalories per mole. McClure also reported that Ni^{+2} in ferrites has an octahedral preference energy which is 22.8 kilocalories per mole greater than that for tetrahedral sites.

Since no other ions, except possibly manganese, have

valence states of approximately equivalent energy, the ions replacing iron in spinels will substitute for either the divalent or trivalent ions, but seldom for both types. This effectively limits the sites among which electrons may be exchanged. In addition, a vacancy may diffuse only by interchanging positions with the neighboring ions in their fixed valence states.

Birchenall goes on to say that "...the hypothesis suggested above is to be used as a guide to the study of the chemistry of diffusion in ferrite crystals. In order to distinguish effects of the sort postulated it is necessary to control the oxygen to metal ion ratio. This has not yet been done in spinel diffusion experiments. Since it is not known how the self-diffusion coefficients depend on the cation-anion ratio it is not clear to what extent the published results for different spinels may be compared with each other."

Although this was true at the time, some progress has been made since then. Schmalzried (28) has determined that the relationship between the self-diffusion coefficient of iron in Fe_3O_4 and the equilibrium oxygen pressure can be expressed as:

$$d \log D_{Fe} = \frac{2}{3} d \log P_{O_2}$$

or

$$D_{Fe} = K (P_{O_2})^{2/3}$$

where D_{Fe} = self-diffusion coefficient of iron

K = constant

P_{O_2} = oxygen partial pressure

Müller and Schmalzried (11) have studied diffusion in cobalt ferrite and have found that for iron contents in excess of the stoichiometric composition, the dependence of the self-diffusion coefficient for both cobalt and iron could be expressed in the same manner as determined by Schmalzried for Fe_3O_4. They were also able to confirm that the diffusion of cobalt occurs by a vacancy mechanism, the Co^{+2} ions moving primarily through the octahedral vacancies in the ferrite structure. Although the same mechanism was postulated for the iron diffusion, they made no specific comments about the diffusion mechanism because of the lack of detailed measurements on iron made in this study.

Sachs (29), in a study of scaling on iron-nickel alloys, determined that nickel is apparently less mobile than iron in the spinel portion of the layer of scale formed on the alloys.

Experimental Results of Solid State Reaction Studies

Solymosi and Szabó (30) determined that spinel formation begins at 650-700°C in $NiO-Fe_2O_3$ mixtures. Beretka and Marriage (31) compared five different techniques for the determination of the initial formation temperature of nickel ferrite spinel. These were magnetic susceptibility, electrical resistivity, x-ray diffraction, thermal gravimetric analysis and differential thermal analysis. They found that the five techniques showed a spread of about 100°C in the detected initial formation temperature, varying from 690°C to 780°C. One of their conclusions was that, while magnetic

susceptibility and x-ray diffraction are not quite as sensitive as the electrical resistivity method, they do enable quantitative information to be obtained about the reaction.

Okamura and Simoizaka (32) mixed NiO and Fe_2O_3 powders in a 1:1 mole ratio, and then reacted pellets of these powders in air under different pressures and at different temperatures for times up to eight hours. They also found spinel formation beginning at about 700°C. Their results are summarized in Figure 4.

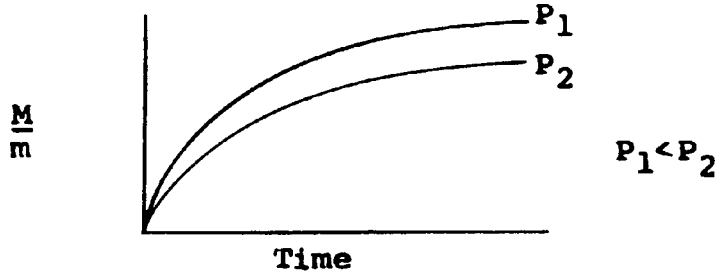


Figure 4. Magnetic Moment per Unit Mass Versus Reaction Time for Nickel Ferrite Formation in Different Atmospheres.

They noted that the "magnetic intensity, finally acquired at a definite temperature, is uniquely decided by the presence of the outside air which is in equilibrium with the sample. Accordingly... the amount of so-called 'impurity' will be found to be a function of the pressure of the outside air." The "impurity" referred to apparently encompasses all the effects due to different oxygen contents in the atmosphere. Several of these effects are discussed later.

Lindner (33) has also shown experimentally that the

formation of $ZnFe_2O_4$ proceeds according to the Wagner mechanism, but that this mechanism was not followed for several other spinels as well as several silicates.

Carter (34) employed inert markers in a study showing that the solid-state reactions forming $MgAl_2O_4$ and $MgFe_2O_4$ occur by counter diffusion of the cations through the relatively rigid oxygen lattice of the product. From this work, he concluded that aluminates and ferrites form by the same mechanism.

Linder and Åkerstrom (35) showed by means of inert markers and radioactively measured reaction constants that the Wagner mechanism appears probable for the formation of chromites, whereas it appears improbable for the formation of aluminates.

Finch and Sinha (36) theorize that crystallographic phase transformations and the formation of transitional superstructures constitute the phase boundary processes in solid state reactions. The crystalline framework of the lattice is maintained throughout the progress of such reactions and the reaction rate is governed by the dynamics of the diffusion process.

For the case of nickel ferrite, Finch and Sinha (37) propose that a necessary first step in the solid-state reaction is the formation of γ-Fe_2O_3, having precisely the same structure as the product, through which the component cations can counterdiffuse to form the ferrite.

Sinha (38) has shown experimentally that the γ-Fe_2O_3

does exist during the formation reaction for nickel ferrite, and concludes that the proposed intermediate step is valid.

Turnbull (18) has analyzed nickel ferrite reaction rate data using Tammann's (39) empirical expression,

$$C = A \log t + B$$

where C = concentration of reaction products

t = time

A, B = constants

He stated that breaks he found in the concentration versus time curves imply a change in the reaction mechanism and, using Huttig's (40) reaction model, he interpreted the breaks as due to three different stages in the reaction mechanism: first, formation of surface layers of nickel ferrite by surface migration of one or more components; second, bulk diffusion, which occurs after a coherent ferrite layer has been formed; third, formation of the final lattice relatively free of defects. This third stage was confirmed by the x-ray measurements of Kedesdy and Katz (41), who showed that the diffraction pattern becomes more perfect with time.

Forestier (42) carried out an extensive study in which he limited his investigations to purely surface reactions. In this way he was able to study the effect of adsorbed gases on the surface reactivity of materials. His method was to study the effect of different atmospheres during formation of ferrites from the component oxides, employing short reaction times and large contact areas in an attempt to avoid the complications of bulk diffusion.

He found that for different types of gases, including H_2O, CO_2, O_2, air, N_2, A, Ne and He, the mechanism of the action of the gas on the formation was the same for all gases, the velocity of formation varies according to the gas adsorbed, and the reaction speed is an increasing function of the temperature of liquefaction of the adsorbed gas, and, thus, a function of the amount of the gas adsorbed. He did, however, note an anomaly in the cases of nitrogen and air which corresponded to a deficiency of adsorption of the gas. He also studied the effect of decreased external pressure on the reaction systems and found that the rate of formation tends toward zero as the pressure tends toward zero.

Forestier explained these results as being due to a decrease of the frequency of vibration of the surface atoms of the solid under the influence of the adsorbed gas, which leads to a relaxation of the bonds between the atoms. This appeared to explain readily the variation of reactivity of the solid according to the nature of the adsorbed gas, and in particular the considerable reactivity in vacuum.

Forestier and Kiehl (43) found that the rate of formation of $NiFe_2O_4$ from NiO and Fe_2O_3 increases logarithmically with the partial pressure of H_2O in the atmosphere over a pressure range of 10^{-5} to 760 millimeters mercury and a temperature range of 500 to 700°C. Extrapolation of their data shows that the rate goes to zero at 10^{-9} millimeters mercury. They also determined that the order in which the gases investigated increasingly accelerate the reaction in

the temperature range 600 to 700°C is He, Ne, N_2, A + O_2, CO_2, and H_2O.

Henrich (44) has studied the effect of varying oxygen pressure on several different formation reactions. The results are summarized below to show that varying the oxygen pressure can have different effects on different systems.

The reaction

$$MgO + Cr_2O_3 \longrightarrow MgCr_2O_4$$

proceeds at a faster rate when there is increased oxygen content in the surrounding atmosphere. Henrich proposed as the reason for this behavior an intermediate reaction system:

$$2\ MgO + Cr_2O_3 + \tfrac{3}{2}\ O_2 \longrightarrow 2\ MgCrO_4$$

$$2\ MgCrO_4 \longrightarrow MgO + MgCr_2O_4 + \tfrac{3}{2}\ O_2.$$

His experimental results offered support to this mechanism.

He found that for the formation of $MgAl_2O_4$ from the component oxides, the formation velocity was not influenced by the oxygen content of the atmosphere.

For the reaction

$$MgO + Fe_2O_3 \longrightarrow MgFe_2O_4$$

the reaction velocity was increased by lowering the oxygen content of the surrounding atmosphere. This tendency was attributed to the fact that the dissociation of Fe_2O_3 is repressed when the oxygen content is increased, as can be seen from the reaction

$$6\ Fe_2O_3 \longrightarrow 4\ Fe_3O_4 + O_2.$$

Simon and Schmidt (45) give 0.5 millimeters mercury for

the equilibrium pressure of this system at 1150°C, and 1.0 millimeter mercury at 1200°C. Henrich's reaction temperature lies considerably below these values, so that it is very unlikely that a marked reduction would occur. He felt that it is conceivable that a small number of energy rich lattice sites on the surface of the samples could be formed, even in an atmosphere which is not analytically detectable, and be converted into Fe_3O_4.

Henrich theorized that the Fe_3O_4 is more reactive than the Fe_2O_3, and, thus, the reaction would proceed at a faster rate when Fe_3O_4 is present. On the contrary, increasing the oxygen content represses the reduction of Fe_2O_3, and would retard the rate of ferrite formation.

Schmalzried (46) conducted a series of experiments with various materials, reacting the component oxides to form different spinels. For

$$2\ CoO + TiO_2 \longrightarrow Co_2TiO_4$$

he found that platinum markers originally located at the interface of the two oxides were found at the CoO-spinel phase boundary after the reaction, if conducted in air, and in the middle of the reaction layer if the reaction atmosphere was one of N_2 carefully purified of O_2. It was noted that the reaction rate in N_2 is smaller than in air.

From these measurements he concluded that in the presence of oxygen, the reaction proceeds by movement of cobalt ions and electrons through the reaction product layer, while the oxygen is transported through the gas phase. In the case of

no oxygen present, the conclusion was that the cations counter-diffuse through the reaction product layer and react at the two interfaces.

The same results and conclusions were also derived for the reaction

$$CoO + Cr_2O_3 \longrightarrow CoCr_2O_4.$$

The results for the reaction

$$CoO + Al_2O_3 \longrightarrow CoAl_2O_4$$

were sufficiently ambiguous that no conclusion could be drawn.

Schmalzried was also able to extend the Wagner Theory for solid state reactions to include his experimental results.

Magnetic Properties

Sakamoto, Asahi and Miyahara (47) discussed the effect of variations in the magnetic moment of $MgFe_2O_4$ due to heat treatment. Actually the cation arrangement of the material is influenced by the heat treatment, and this leads to variations in the magnetic properties as discussed by Néel (48, 49). Experimental results showed that the samples are in thermal equilibrium down to a temperature of about 750°C (cooled from 1100°C). Thus, room temperature measurements do not measure the properties due to the high temperature cation arrangements, but those for some intermediate temperature.

Epstein and Frackiewicz (50) also studied the cation distribution in $MgFe_2O_4$ as a function of temperature. Their

results were essentially the same as those of Sakamoto, Asahi and Miyahara regarding cation distribution. Epstein and Frackiewicz note that an increase of the cation concentration in the tetrahedral positions increases the saturation magnetic moment.

Economos (51) also discusses the manner in which heat treatment affects the magnetic moment of $MgFe_2O_4$ due to its effect on the cation distribution. In the true normal and inverse spinel distributions, the magnetic moment is zero. In the actual case, where the cation distribution as a function of heat treatment is intermediate between the two extremes, the net magnetic moment approaches $\frac{2}{3}\mu$ Bohr magnetons, where $\mu = 5$ for $MgFe_2O_4$. The reason for this deviation from ideality is that the cations assume a random distribution on the available sites, resulting in an intermediate-type spinel, in which case the magnetic forces due to the spinning electrons associated with the cations on different sites are not cancelled out.

Jefferson and Grimes (52) compared magnetic and x-ray measurements for the nickel ferrite formation, and found that at a temperature of 1210°C the x-ray measurements showed essentially complete ferrite formation in about three minutes, while the magnetic moment per unit mass continued to change for as long as 900 minutes. They concluded that evidence of reasonably complete spinel structure formation is insufficient evidence for completion of the final magnetic properties of ferrites, also concluding that line sharpness

on the diffraction patterns is more closely related to the magnetic properties. This is in accordance with the results of Turnbull (18) and Kedesdy and Katz (41).

EXPERIMENTAL EQUIPMENT, PROCEDURES AND MATERIALS

This section is devoted to a discussion of the experimental aspects of the study. The descriptions of the equipment are detailed in the case of those pieces specially constructed for this work, but are limited to specifications rather than details where the equipment is of standard design. Some comments are offered on the effect of using different sources of raw materials at different stages of the work, and the materials sources are identified.

Rather than discussing all the numerous and varied methods of specimen preparation and analysis, only those which were the most successful, and were consequently used in the study, are discussed here.

Experimental Equipment

Furnace

The furnace used for the bulk of the experimental work was a double-wound tube furnace with an on-off type temperature controller. The outer winding was of chromel resistance wire wound on an eight-inch diameter ceramic cylinder. The inner coil was of 0.025-inch diameter platinum resistance wire wound on the outside of a one-inch inside diameter alumina furnace tube 24 inches long.

Power was supplied continuously to the outer coil during the operation of the furnace to lighten the load on the inner coil due to heat losses. Power to the inner coil was

supplied intermittently to control the temperature at the desired level. A control thermocouple of Pt-Pt + 13% Rh, located in the hot zone of the furnace, was connected to a Foxboro potentiometer controller which regulated the power supplied to the furnace. The controller settings were based on readings made on a Minneapolis-Honeywell potentiometer attached to a similar thermocouple similarly placed.

Control of the furnace temperature was maintained within about ±2°C. The hot zone of the furnace contained a region about one and one-half inches long over which the temperature fell off a maximum of about 3°C at the ends. It was in this region of flat temperature profile that the samples were placed during firing.

The samples were set on a sheet of platinum foil shaped to fit the furnace tube before being inserted in the hot zone of the furnace.

Electron Microprobe

The quantitative analytical work on the diffusion couple-type specimens was done with an electron microprobe through the courtesy of the Scientific Laboratories of the Ford Motor Company and the General Atomic Division of General Dynamics Corporation.

Faraday Balance

Magnetic moments of the reacted samples were measured on a Faraday balance, which consists of an electromagnet capable of producing a gradient magnetic field, a means of suspending a sample in this gradient field, and a means of

measuring the force exerted on the sample by the magnetic field.

For this work, the Faraday balance consisted of a four-inch Varian electromagnet with regulated power supply, and an analytical beam balance, to which was attached a sample holder on a chain which hung down into the magnetic field. The chain was attached to one balance pan, while calibrated weights were placed on the other pan to determine the force on the unknown sample.

X-Ray Facilities

The quantitative x-ray fluorescent analyses were made using a Norelco x-ray fluorescent analyzer. A LiF diffraction crystal was used. Intensities of the diffracted beams were measured by an electronic scintillation counter attached to an automatic recorder.

The lattice parameter determinations were made using a 114.6 millimeter Debye-Scherrer diffraction camera mounted on a Norelco x-ray source. Cobalt radiation was used with an iron filter.

Materials

The underlying thought in selecting raw materials for use in this study was that the only variables desired were reaction time, temperature and oxygen partial pressure. Thus it was necessary to control all the other possible variables. The simplest way to do this seemed to be by using materials from the same source. Since this was not entirely possible, it was deemed sufficient to use similar starting materials

for all tests compared among themselves. For example, all conversion tests run at 1200°C were made using samples from the same batch of 1:1 NiO to Fe_2O_3 mixture, and only the atmosphere and time were varied. However, it was thought acceptable to perform the 750°C and 1200°C tests using different sources of starting materials, since the two sets of data were not directly compared with each other; only the relative results of each set of samples were compared. Since the tests run at 750°C were the preliminary experiments which led to the rest of the work, the same starting materials were not available for the 1200°C tests. Thus it was necessary to use materials as near the same as possible.

The NiO used throughout most of the study was reagent grade powder (CB 918, NX 345) manufactured by the Matheson Coleman and Bell division of the Matheson Company, Inc. The Fe_2O_3 used was reagent grade powder (Code 1741) manufactured by the General Chemical Division of Allied Chemical Company.

The atmospheres used in the experiments were supplied by flowing pre-mixed gases through the furnace. 100% O_2 was obtained from the General Stores of the University. Compressed air was used for the 21% O_2 source. 1% O_2 in N_2 was obtained from the Matheson Company.

It is evident from the variations in results achieved after only five minutes (see Figure 5) that this method of atmosphere control is quite effective. Table I lists the results of mass spectrographic analyses made on samples of the furnace atmosphere taken at different times. These

analyses confirm that the furnace atmosphere actually was that which was desired.

Table I

Furnace Atmosphere Analysis

Time Elapsed While Gas Flowing	Oxygen Content of Feed	Analysis	
		Oxygen	Nitrogen
2 hours	1.05%	1.11%	98.89%
6 hours	1.05%	1.03%	98.97%
28 hours	1.05%	1.05%	98.95%
100 hours	1.05%	1.22%	98.78%
2 hours	100.00%	100%	(better than O_2 standard)
6 hours	100.00%	98.49%	1.51%

The atmosphere was passed through a drying column containing activated alumina, and then through indicating Drierite, thus assuring a maximum dew point of -40°C. Flow rate was monitored by passing the exit gases through a bubble flow meter. Samples for gas analysis were taken by inserting a sample tube in the line between the furnace and flow meter.

Specimen Preparation, Treatment and Analysis

Diffusion Couples

The first step in forming the diffusion couples for this study was to press Fe_2O_3 into pellets 3/8 inches in diameter,

using ethyl ether as a binder and pressing just hard enough to produce a firm pellet. These pellets were then sintered by raising the temperature slowly to 1100°C and holding the samples at this temperature for 24 hours in air, after which they were cooled slowly to room temperature.

After placing 0.0008-inch diameter platinum wire on the surface of the Fe_2O_3 pellets, NiO was then pressed around the Fe_2O_3, using ethyl ether as a binder and pressing to about 15000 psi in a 3/4-inch diameter die.

These couples were then placed in the hot zone of the furnace, atmosphere control was begun, and the furnace temperature was raised slowly to the desired level to avoid cracking of the couples due to thermal shock.

After four days at temperature the samples were quenched either with forced air or with water. It was found necessary to water quench the samples fired in 1% O_2 to suppress precipitation of Fe_2O_3 from the ferrite near the Fe_2O_3-ferrite boundary.

The couples were then mounted in room-temperature-setting plastic and polished through one-micron diamond compound. A layer of carbon was vacuum deposited to prevent charge-buildup during the electron microprobe analysis.

The microprobe analysis was performed by analyzing for cation concentration along a line through the NiO, ferrite product layer, and the Fe_2O_3. The data were obtained by use of a recorder readout system. This results in a

graphical presentation of the data, and, while this method is only semi-quantitative, it is estimated that the accuracy in this application is about ±1% on the nickel analysis and ±3% on the iron analysis. Calibration of the equipment was accomplished by analyzing a series of nickel ferrites of various compositions which were supplied by the Bell Telephone Laboratories, Murray Hill, New Jersey.

Reaction Rate Samples

A mixture of Fe_2O_3 and NiO in a 1:1 mole ratio was thoroughly mixed by shaking the mixture in ethyl ether. Pellets were then formed by pressing the mixture in a 3/8-inch diameter die at about 15,000 psi. Pellet height was generally about 1/4 inch.

The pellets were placed in the cold end of the furnace tube, the tube closed, and gas passed through the furnace for fifteen minutes before insertion of the samples in the hot zone to allow purging of the furnace and supplying of the desired atmosphere for the experiment. When the samples were moved into the hot zone, the furnace temperature dropped, but invariably returned to the preset value within about two minutes.

After the samples had been in the hot zone for the desired length of time, they were removed and cooled by forced air. Analysis by x-ray diffraction revealed no Fe_2O_3 present in the three-hour sample fired in 1% O_2, indicating that cooling was rapid enough to prevent precipitation of Fe_2O_3 from the ferrite during cooling.

The samples were then ground to -100 mesh, weighed to the nearest 0.1 milligram, and the magnetic moment determined to the nearest milligram.

Since it was very difficult to reproduce the magnetic field precisely, all magnetic moments were determined during the same session in order to insure the same conditions of measurement. A different Faraday balance was used for measuring the 750°C samples; thus, the measurements of these samples cannot be compared quantitatively with any of the others.

Lattice Parameters

Samples for lattice parameter determination were ground to -100 mesh and placed in 0.3 millimeter glass capillary tubes. X-ray diffraction patterns were made using a 114.6 millimeter diameter cylindrical Debye-Scherrer camera with cobalt radiation and an iron filter. Best results were obtained using an operating voltage of forty kilovolts, a filament current of ten milliamperes and an exposure time of four hours.

Analysis of the powder patterns obtained was carried out using Gluck's (5) computer program.

X-Ray Fluorescence

The chemical analysis of the nickel ferrite standards supplied by Bell Labs was checked using x-ray fluorescent analysis. Mixtures of Fe_2O_3 and NiO were prepared to give ferrites of 5, 10, 15 and 20 weight per cent nickel when fired.

These samples, as well as small portions of the Bell Labs samples, were then ground to -100 mesh and analyzed using the x-ray fluorescent equipment described earlier. Since the samples were in powder form, it was deemed sufficient to evaluate the samples on the basis of ratios of peak heights or areas under the diffractometer curves, rather than working with absolute compositions. In this way errors due to different packing densities, amounts of samples, etc., were avoided.

The results of these analyses are shown in Table A-I and Figures A-1 and A-2, and they indicate that the compositions supplied by Bell Labs were as stated; thus it was assumed that these compositions were accurate.

RESULTS

Reaction Rate Samples

1. Curves of magnetic moment per unit mass versus reaction time for periods up to three hours in different furnace atmospheres at 1200°C for a 1:1 mole ratio of NiO and Fe_2O_3 are shown in Figure 5.
2. Curves of magnetic moment per unit mass versus reaction time for periods up to sixteen hours in different furnace atmospheres at 750°C for a 1:1 mole ratio of NiO and Fe_2O_3 are shown in Figure 6.
3. The reaction rate data obtained at 750°C are shown in Figure 7, using the Jander equation (18) to present the data.
4. The reaction rate data obtained at 750°C are shown in Figure 8, using the equation of Ginstling and Brounshtein (16) to present the data.
5. Curves of magnetic moment per unit mass versus reaction time for periods up to 42 days in different temperatures for a 1:1 mole ratio of NiO and Fe_2O_3 are shown in Figure 9.

Rate of Consumption of Reactants

Analysis of Debye-Scherrer x-ray powder patterns showed that after reacting a 1:1 mole ratio of NiO and Fe_2O_3 for three hours at 1200°C in 100% O_2, there was still Fe_2O_3 present. Firing under the same conditions in 1% O_2 resulted in complete disappearance of the Fe_2O_3.

Changes in Average Lattice Parameter of Nickel Ferrite

Plots of the average lattice parameter of nickel ferrite formed by reacting a 1:1 mole ratio of NiO and Fe_2O_3 are shown in Figures 10 to 12 as a function of reaction time at different temperatures and in different atmospheres. The plots include an estimate of the standard deviation for each measurement.

Concentration Profiles in Diffusion Couples

Cation concentration profiles across the nickel ferrite product layer of diffusion couple-type samples fired at 1200°C in atmospheres of various oxygen contents are shown in Figures 13 to 15.

Inert Marker Measurements

Platinum wire markers placed at the original interface in the diffusion couples were found near the middle of the product layer in all three cases of different firing atmospheres at 1200°C.

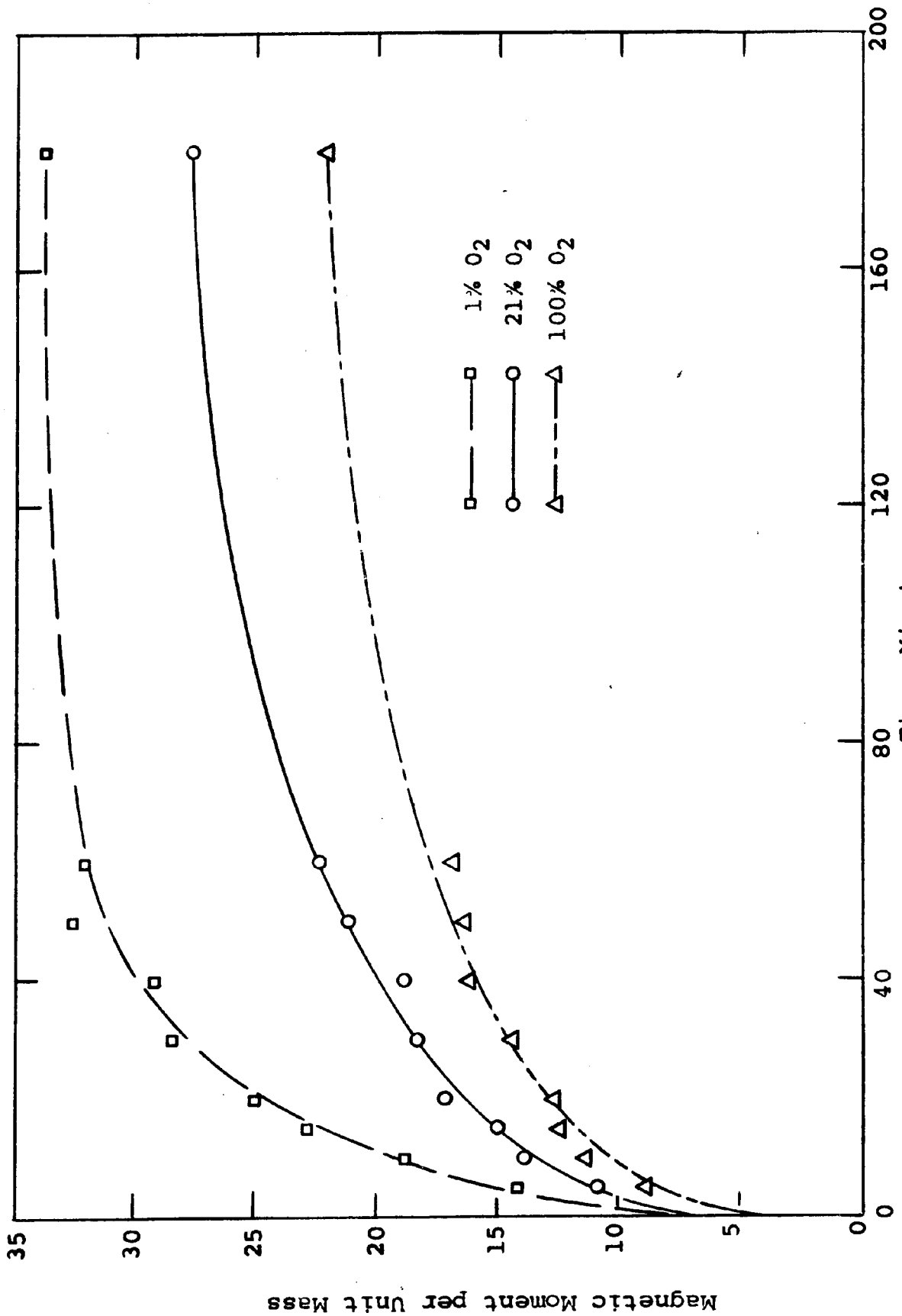


Figure 5. Magnetic Moment per Unit Mass Versus Reaction Time for 1:1 Mole Ratio NiO and Fe_2O_3 Samples in Different Atmospheres at 1200°C.

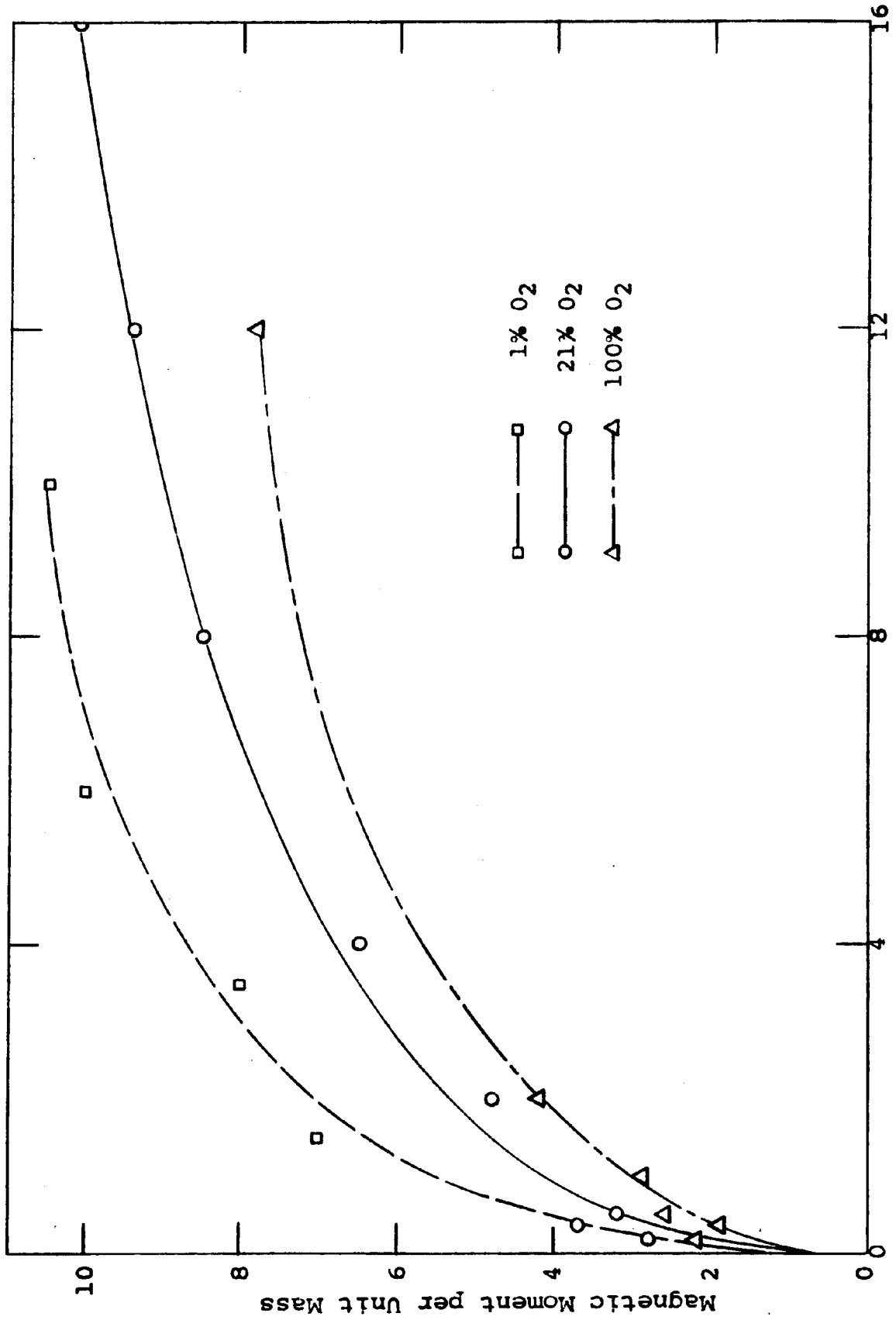


Figure 6. Magnetic Moment per Unit Mass Versus Reaction Time for 1:1 Mole Ratio NiO and Fe_2O_3 Samples in Different Atmospheres at 750°C.

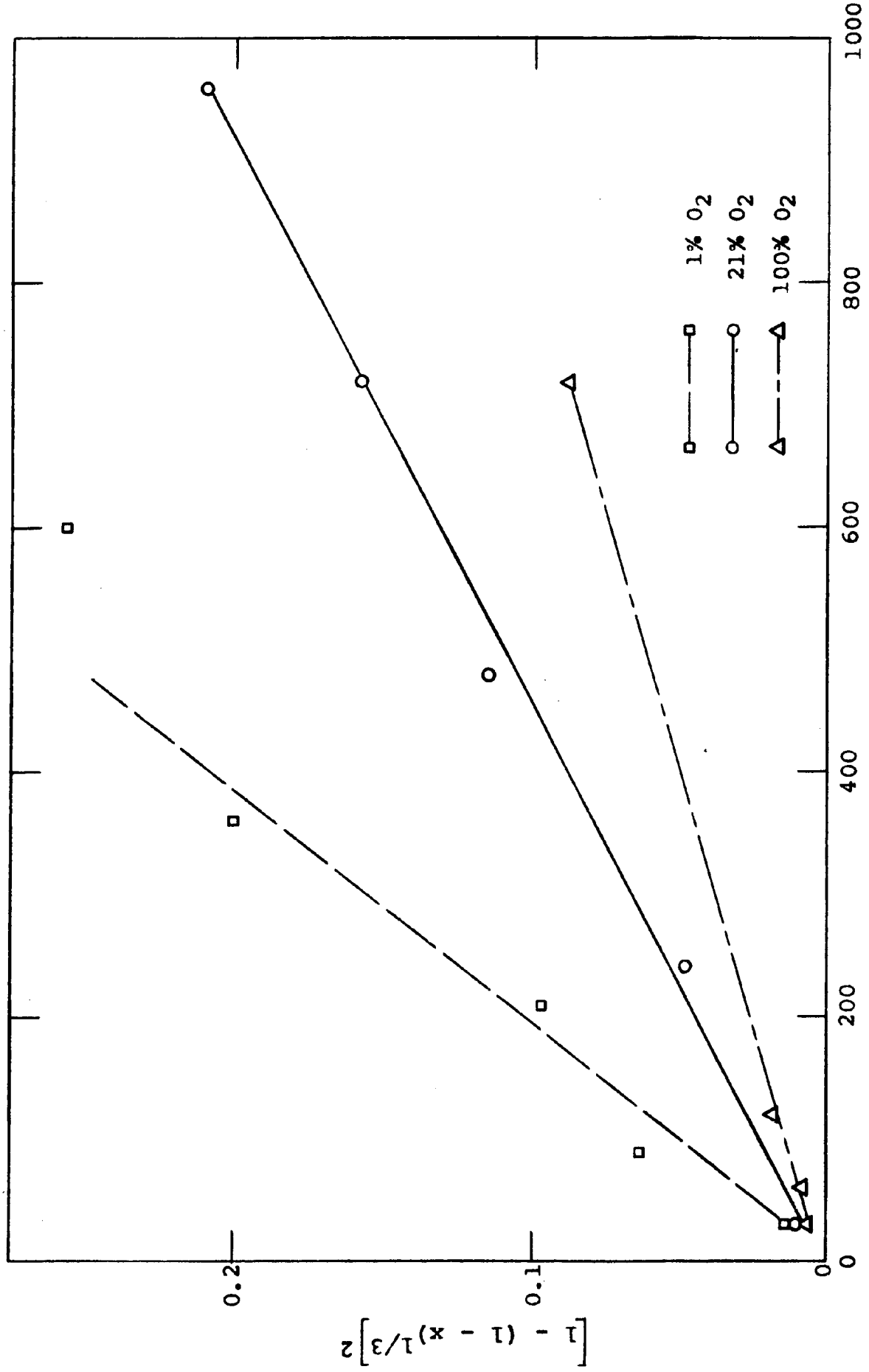


Figure 7. Jander Plot of 750°C Reaction Rate Data on 1:1 Mole Ratio NiO and Fe_2O_3 Samples at 750°C.

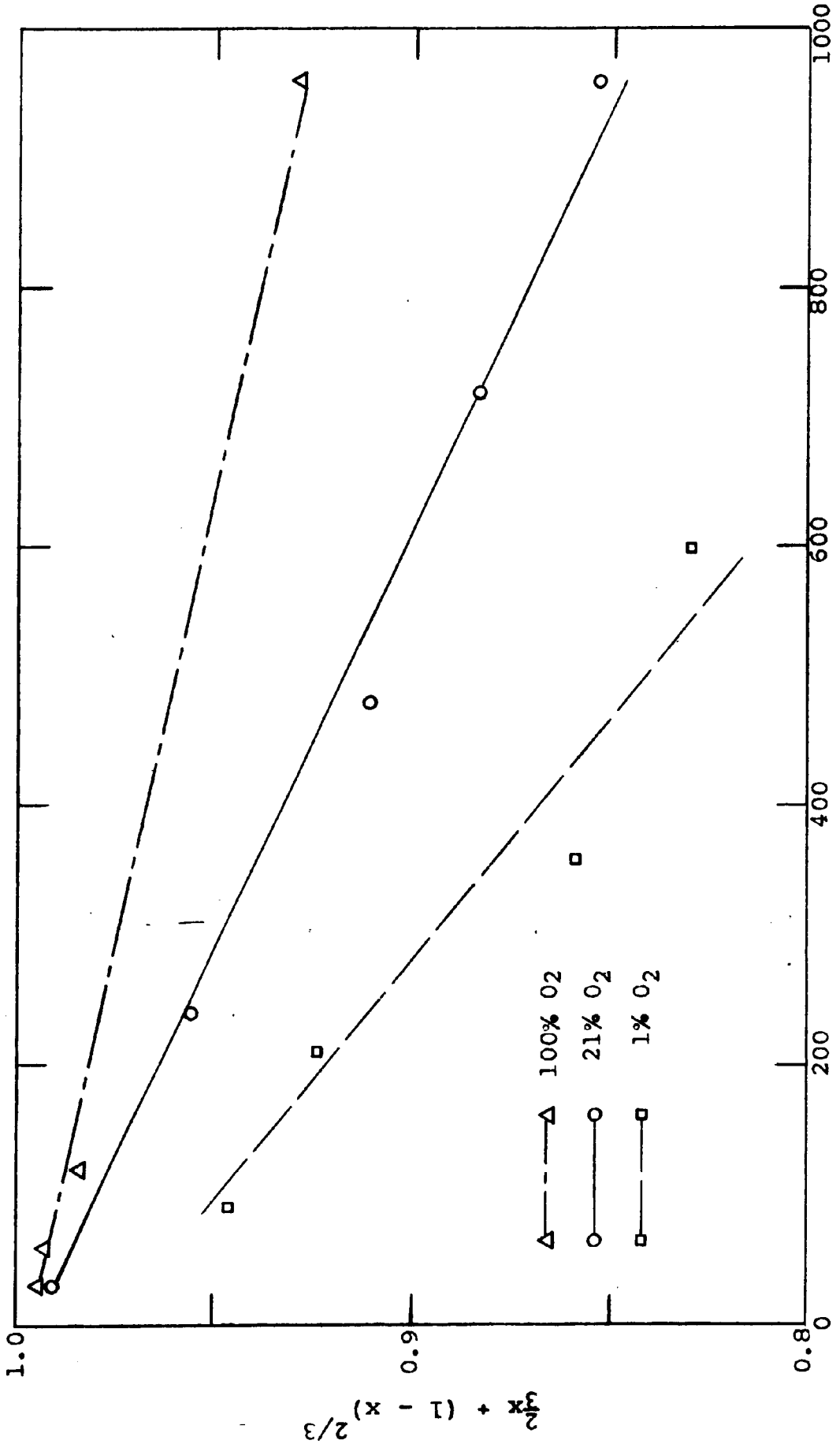


Figure 8. Ginstling - Brounshtein Plot of Reaction Rate Data on 1:1 Mole Ratio NiO and Fe_2O_3 Samples at 750°C

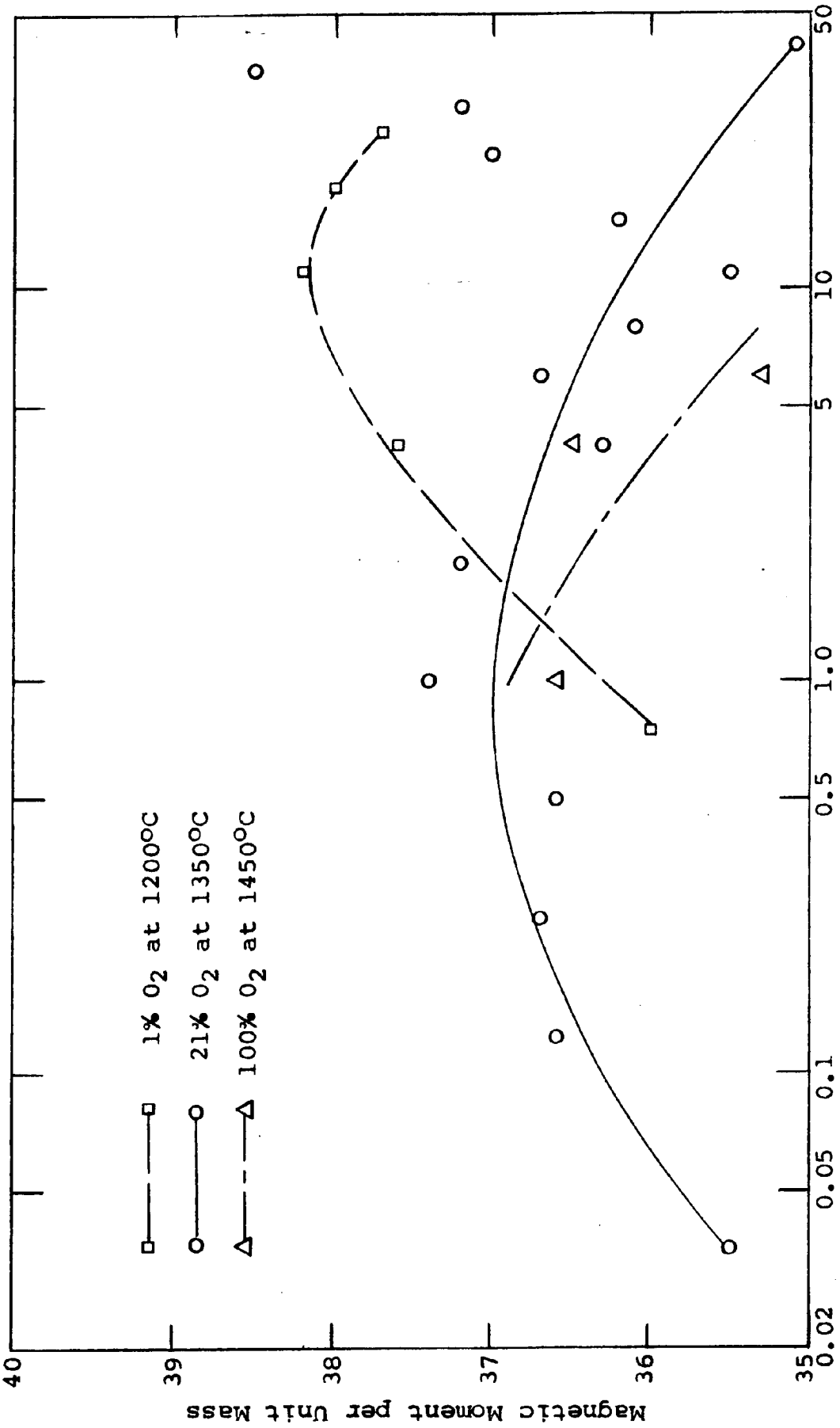


Figure 9. Magnetic Moment versus Reaction Time for 1:1 Mole Ratio of NiO and Fe_2O_3

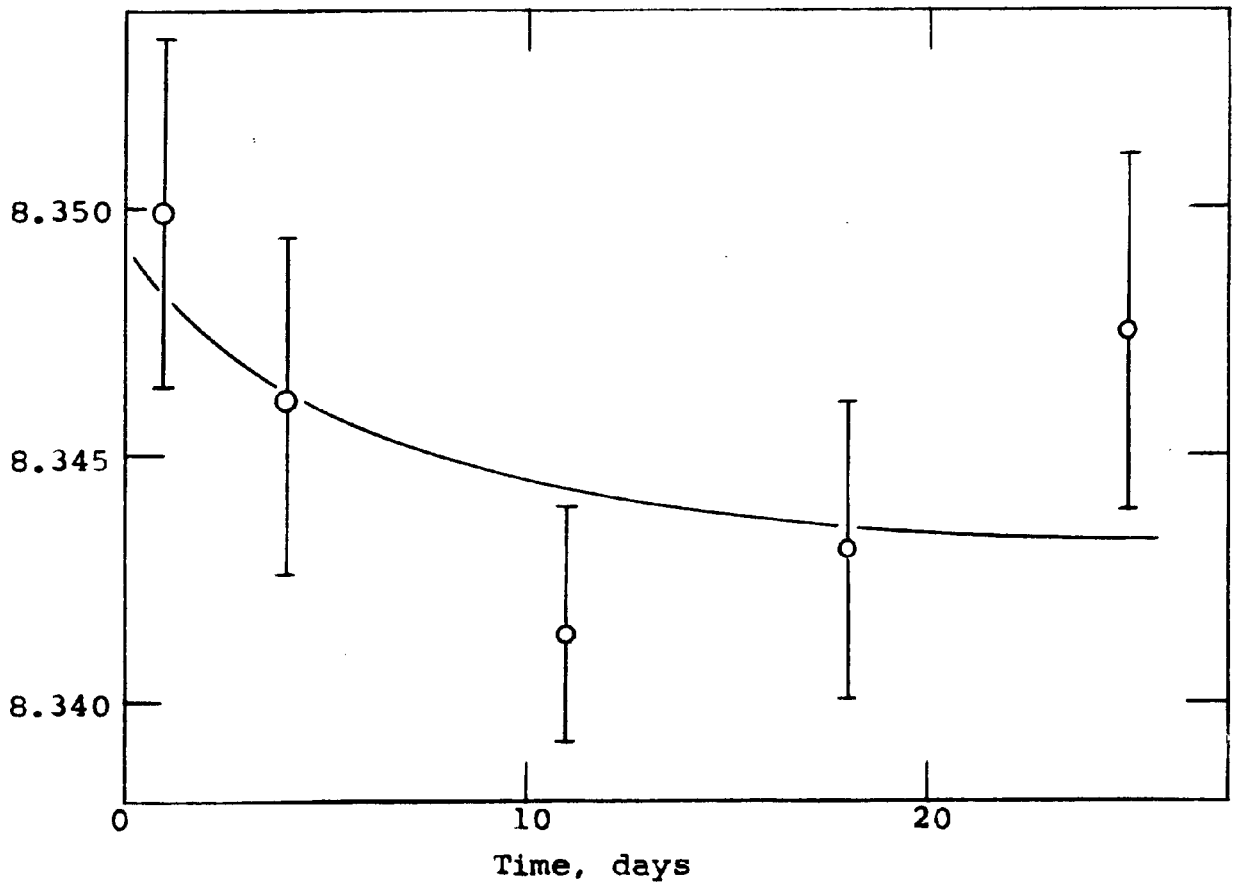


Figure 10. Average Lattice Parameter Versus Reaction Time for Nickel Ferrite Fired in 1% O_2 at 1200°C.

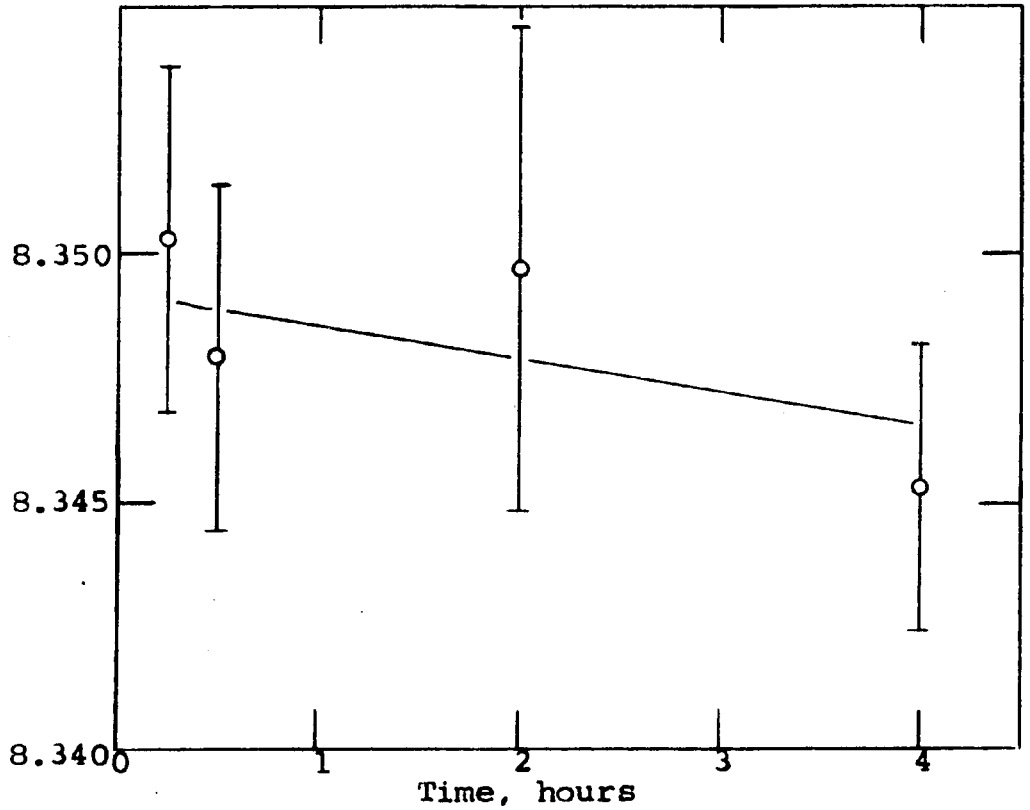


Figure 11. Average Lattice Parameter Versus Reaction Time for Nickel Ferrite Fired in 1% O_2 at 1300°C

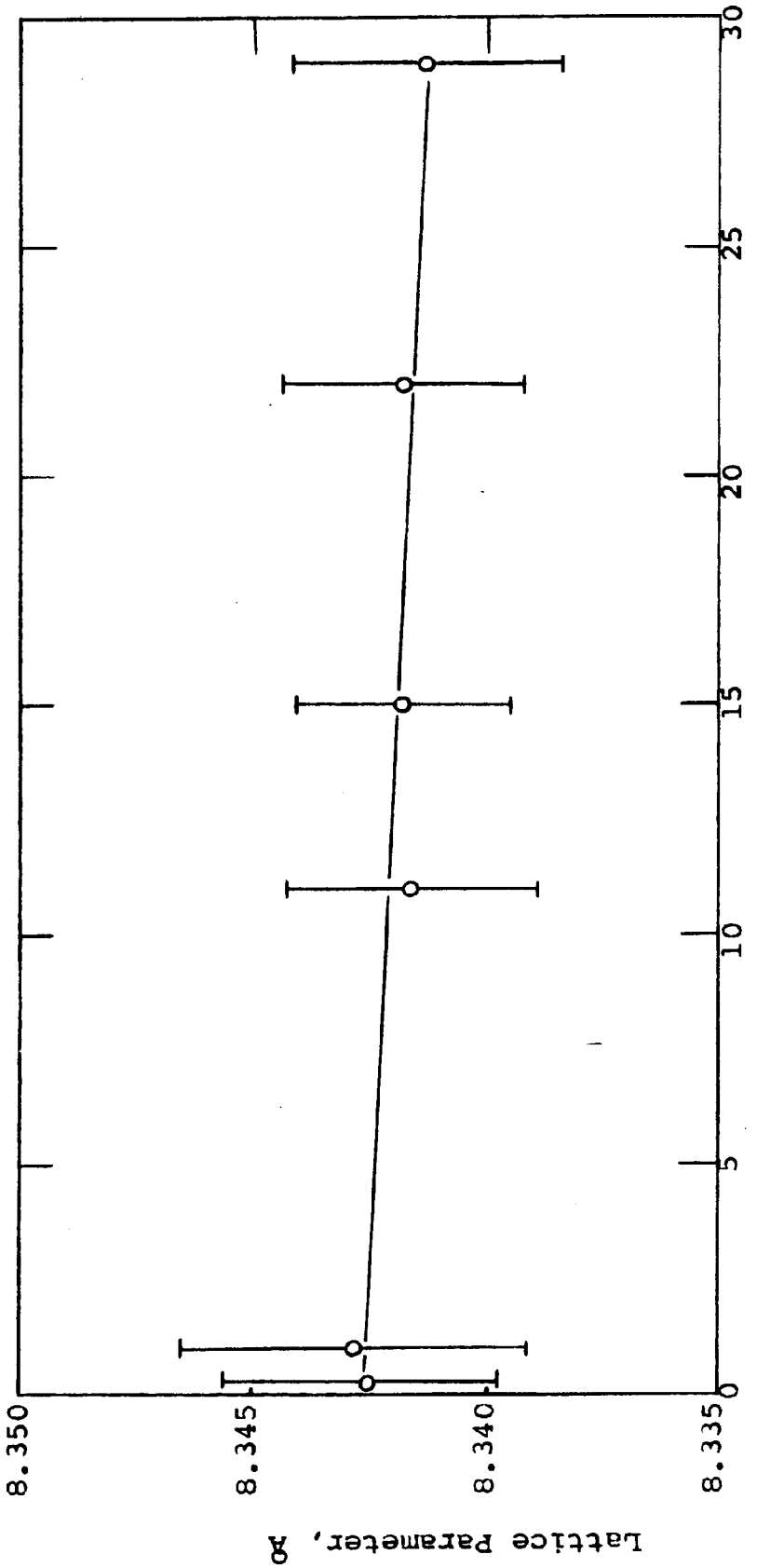


Figure 12. Average Lattice Parameter Versus Reaction Time for Nickel Ferrite Fired in 21% O_2 at 1350°C.

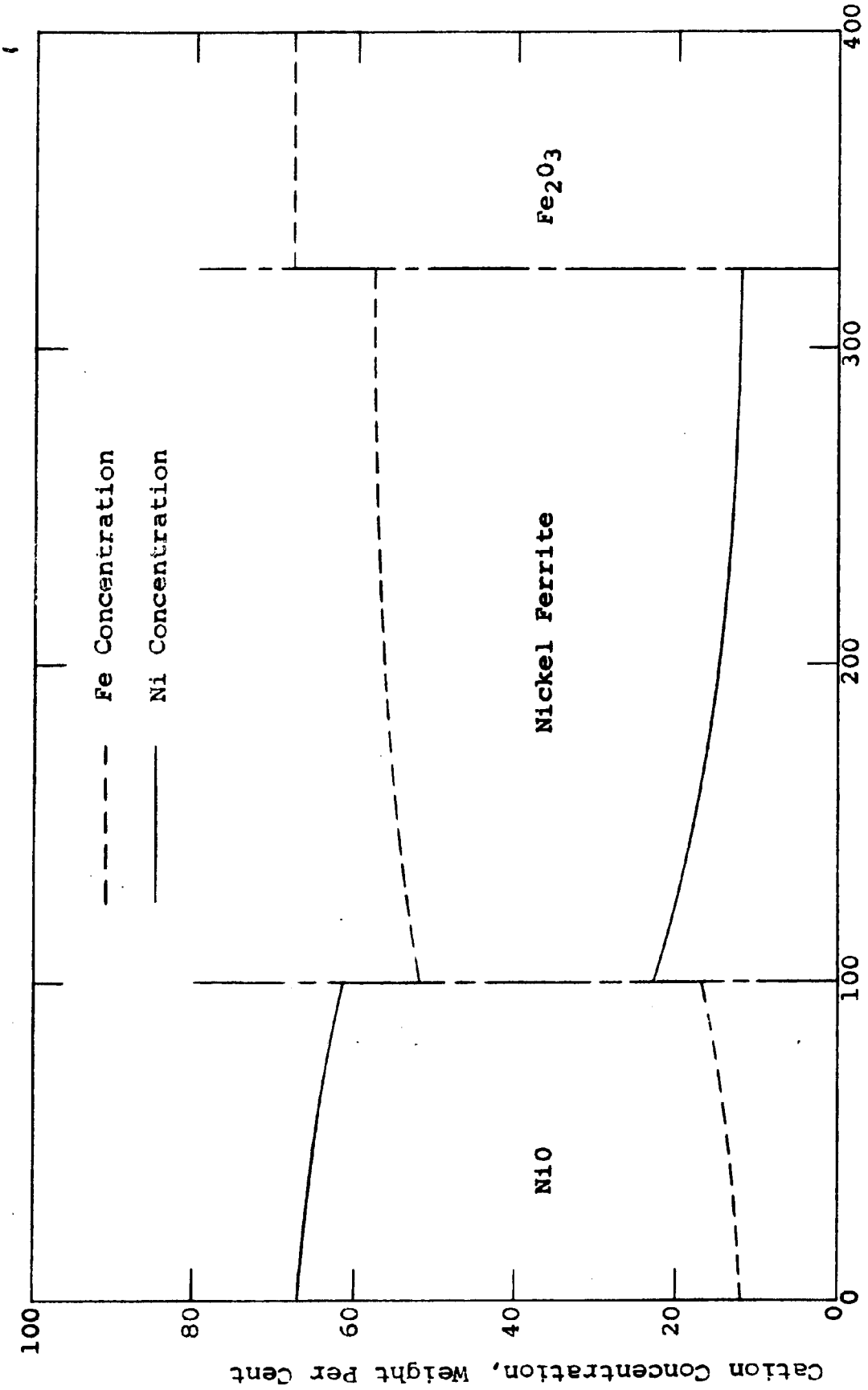


Figure 13. Cation Concentration Profiles in NiO - Fe_2O_3 Diffusion Couple Reacted Four Days in 100% O_2 at 1200°C

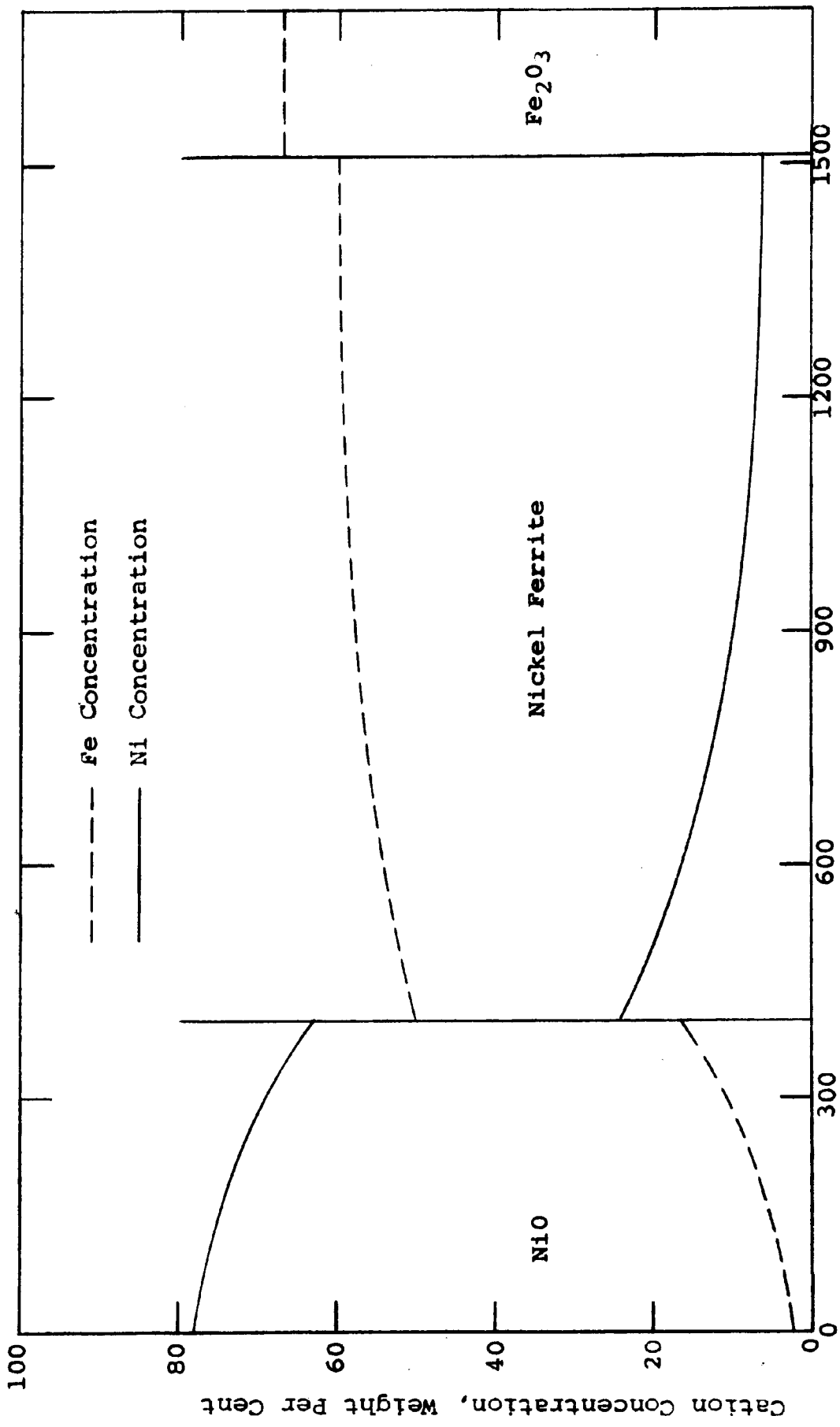


Figure 14. Cation Concentration Profiles in NiO - Fe_2O_3 Diffusion Couple Reacted Four Days in 21% O_2 at 1200°C

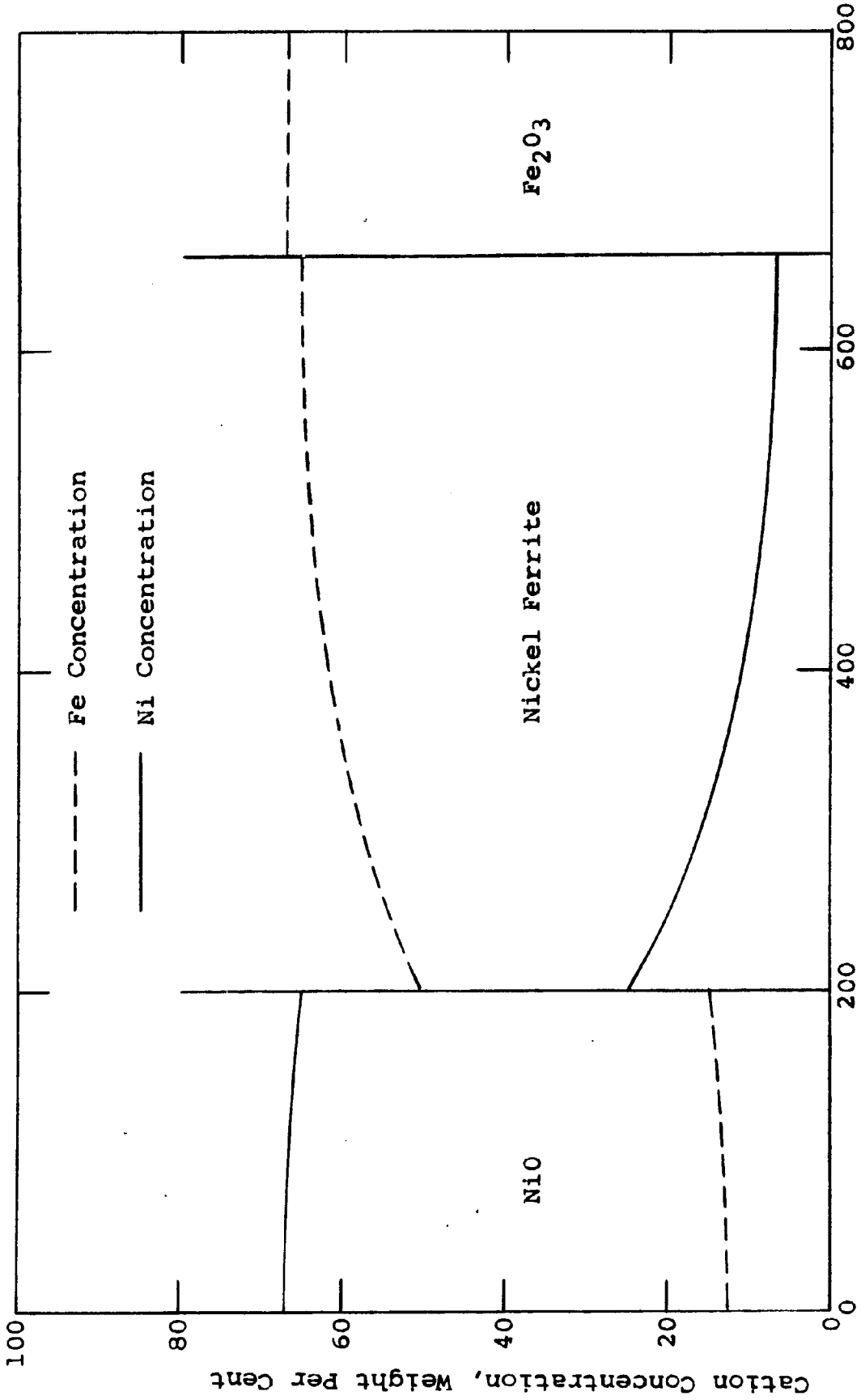


Figure 15. Cation Concentration Profiles in NiO - Fe_2O_3 Diffusion Couple Reacted Four Days in 1% O_2 at 1200°C

ANALYSIS OF RESULTS

While this section contains some discussion of the experimental results obtained, it is devoted primarily to the phenomenological description of the reaction process. The order of discussion of the different topics has been arranged so that information and concepts necessary for the discussion of any topic are provided prior to that discussion.

The first topic, the cation concentration profiles, is concerned mainly with a description of the different effects contributing to the shape of the concentration profiles. Some discussion is also included to relate these concentration profiles to the reaction rates observed.

The second topic, the actual formation of the ferrite product, considers modifications in the mechanism proposed by Wagner (1, 2) to bring his mechanism into agreement with the results obtained in this study.

The next topic covers all those matters related to the magnetic moment measurements. The reasons for the different appearances of the short- and long-time reaction curves are discussed. This includes the interrelationship of furnace atmosphere, composition variations in the product, and resultant variations in magnetic moment. The differences between the two groups of curves are discussed, and the reconciliation of the two is accomplished. The relationship between the magnetic moment measurement and the actual material being measured is also discussed.

The shift in the average lattice parameter of the ferrite with reaction time is related to the composition changes occurring. Finally the knowledge gained in the course of this study is applied to the prediction of the optimum conditions for conduct of the reaction.

Cation Concentration Profiles

Since one of the objects of this study was to investigate the effects of concentration gradients on the rate of nickel ferrite formation, it was desired to work at a temperature which resulted in the greatest variation in composition. Examination of the phase diagram showed that 1200°C was the highest convenient temperature at which all the oxygen isobars emerged from the ferrite region within the ternary system, rather than extending into the Fe_3O_4(SS) region in the Fe-O boundary. Thus, this temperature was selected for the bulk of the experimental work.

The cation concentration profiles across the nickel ferrite product layer in the diffusion couples prepared in different atmospheres (Figures 13 to 15) are in good agreement at the NiO-ferrite interface with the values predicted by the phase diagram, if equilibrium between the NiO and ferrite is assumed (see Table II). The agreement between measured and predicted values at the Fe_2O_3-ferrite interface is not good in two of the three samples.

This lack of agreement at the Fe_2O_3-ferrite interface seems to imply that perhaps the assumption of equilibrium at that interface is not valid. One possible contributing

Table II

Interface Compositions in Diffusion Couples at 1200°C*

Reaction Atmosphere	NiO-ferrite Boundary Predicted	NiO-ferrite Boundary Experimental	Fe_2O_3-ferrite Boundary Predicted	Fe_2O_3-ferrite Boundary Experimental
100% O_2	24.6 Ni	25 Ni	20.8 Ni	12 Ni
	48.2 Fe	52 Fe	51.3 Fe	58 Fe
21% O_2	24.6 Ni	25 Ni	18.1 Ni	7 Ni
	48.2 Fe	50 Fe	54.4 Fe	60 Fe
1% O_2	24.6 Ni	25 Ni	7.1 Ni	7 Ni
	48.2 Fe	50 Fe	65.3 Fe	65 Fe

*All compositions expressed as weight per cent

factor to this situation may be that the reactants are affected by a surface condition, such as adsorbed gases, to such an extent that equilibrium is unattainable at this interface.

It is of considerable interest to examine the shapes of the concentration profiles. In all three cases they are steep near the NiO-ferrite interface and level off towards the Fe_2O_3-ferrite interface. Thus a considerable portion of the ferrite layer consists of material which has, relative to the ferrite at the NiO-ferrite interface, a high iron and a low nickel concentration, i.e., a high iron-to-nickel ratio. The explanation for these results lies in a consideration of the overall compositions as one moves through the product layer.

Referring to the sketches of Figure 16, we see that at the NiO-ferrite interface we have (Ni, Fe)O in equilibrium with ferrite of composition A. As we cross the ferrite product layer toward the Fe_2O_3-ferrite interface, both the iron and nickel concentrations change, until we reach the Fe_2O_3-ferrite interface, where we have Fe_2O_3 in contact with nickel ferrite of composition B. Since the iron and nickel concentrations at any point in the ferrite layer are related to the point on the phase diagram representing that iron-to-nickel ratio and the equilibrium oxygen pressure in the atmosphere, the oxygen content of the ferrite at that point is thus specified. We see then that as the iron-to-nickel ratio changes as we proceed across the sample, the oxygen content of the corresponding ferrite changes as determined by the equilibrium with the atmosphere.

Since the cation vacancy concentration is directly related to the excess oxygen content, we see that there is a variation in vacancy concentration across the product layer dependent on the iron-to-nickel ratio and the oxygen partial pressure. Near the NiO-ferrite interface we have a low iron-to-nickel ratio, and from the phase diagram we see that there is only a very small amount of excess oxygen in the ferrite. Moving away from this interface into the ferrite product, the iron-to-nickel ratio increases, as does the excess oxygen content. Thus, the cation vacancy concentration is also increasing as the iron-to-nickel ratio increases.

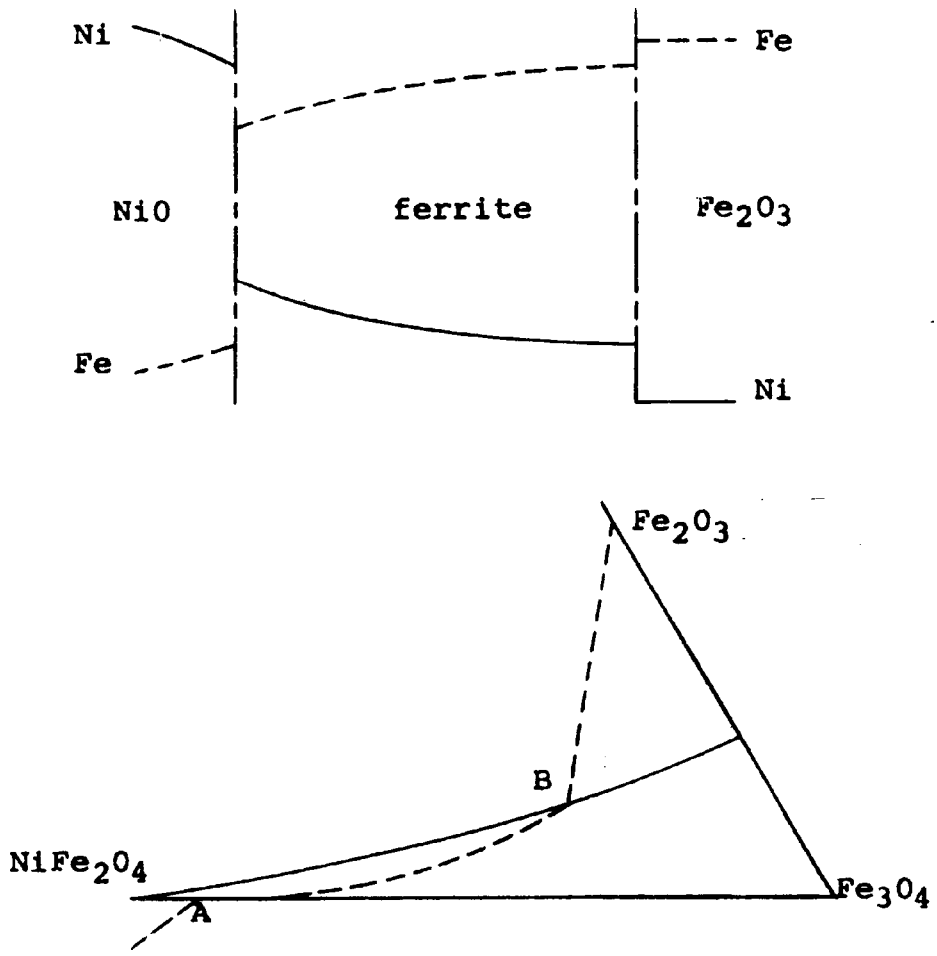


Figure 16. Cation Concentration Profiles Across Product-Reactant Interfaces. Ferrite Portion of Fe-Ni-O Phase Diagram.

In the actual concentration profiles, the slope of the curves changes rapidly near the NiO-ferrite boundary, but the rate of change in slope decreases until, somewhere near the center of the ferrite layer, both the iron and nickel curves have become nearly level. The reason for this behavior lies in the effect of the vacancy concentration on the relative cation diffusivities in different regions of the product layer.

In the regions of low iron-to-nickel ratio, the vacancy

concentration is low and thus the cation diffusivities will be relatively small. Since cation movements are slow, any concentration gradients present will be slow to level out. In the regions of higher iron-to-nickel ratio, the vacancy concentration is higher and thus the cation diffusivities are higher. The faster cation movement in these regions will enable any gradients to level out faster than in the regions of low iron-to-nickel ratio.

To relate this effect to the rate of product formation, we now refer to Figure 17. The distance designated Δc represents a constant excess oxygen concentration, compared to the stoichiometric ferrite, in the samples reacted in different atmospheres, and thus comparable variations in cation vacancy concentration. At the NiO-ferrite interface the iron and nickel concentrations in the ferrite, $\underline{a}_o$ and $\underline{b}_o$ are essentially the same in any atmosphere. However, at the excess oxygen content represented by Δc, the sample fired in 100% O_2 has a composition represented by point $\underline{a}$, while the composition of the 1% O_2 sample is represented by point $\underline{b}$. Relating this to relative compositions, the nickel concentration has decreased from $\underline{b}_o$ to $\underline{b}$ in the 1% O_2 sample and from $\underline{a}_o$ to $\underline{a}$ in the 100% O_2 case, while the iron concentration has increased from $\underline{b}_o$ to $\underline{b}$ in the 1% O_2 case and from $\underline{a}_o$ to $\underline{a}$ in the 100% O_2 case. Thus the concentration differences of both iron and nickel are greater in the 1% O_2 case than in the 100% O_2 case for comparable variations in cation vacancy concentration. For similar product layer

thicknesses, the concentration gradient would be greater in 1% O_2 than in 100% O_2.

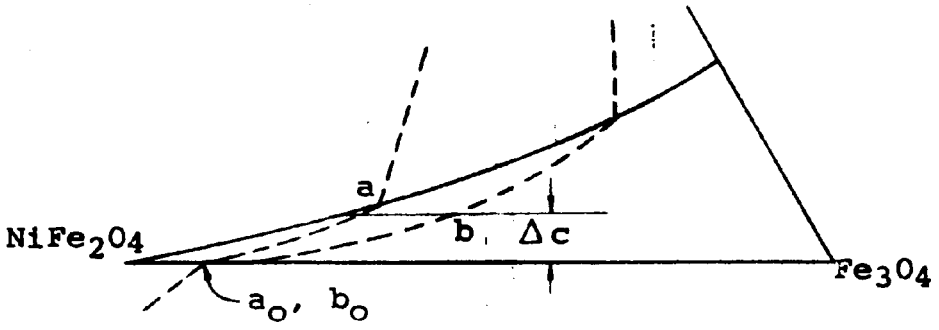
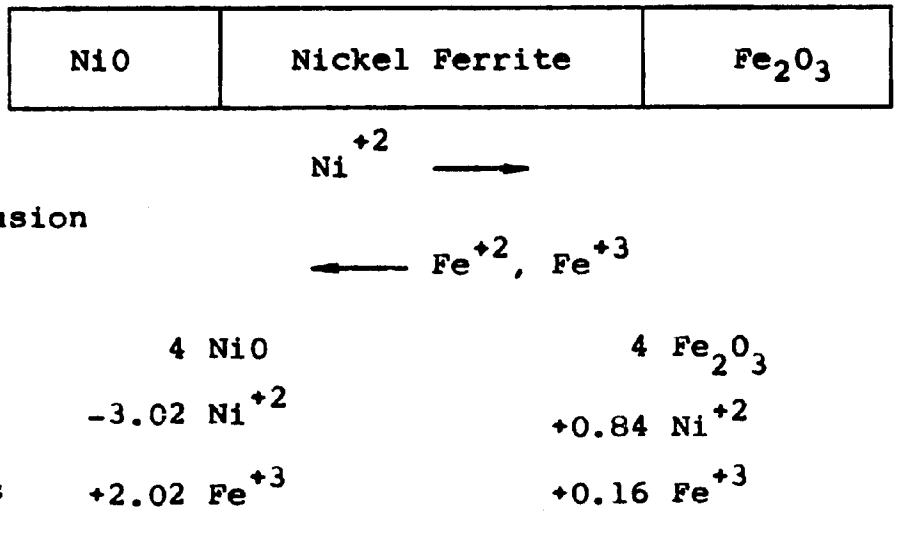


Figure 17. Ferrite Portion of Fe-Ni-O Phase Diagram

Since we have a greater driving force due to concentration gradient in the 1% O_2 case than in the 100% O_2 case over regions of comparable resistance (comparable cation vacancy concentrations), we can expect a faster cation transport through the product layer in the 1% O_2 case, and thus a faster reaction rate than in the 100% O_2 case.

Formation of Ferrite Product

Regarding the formation of the ferrite product, we have situations at the two interfaces which, although similar, have some significant differences. In discussing these data, we shall refer back to the discussion of the Wagner hypothesis in the Literature Survey. The diagram of that discussion is reproduced here, with the coefficients for some of the terms used in describing the reaction process altered to correspond to the situation existing during reaction in a 1% O_2 atmosphere at 1200°C.



Phase	4 NiO	4 Fe_2O_3
Boundary	$-3.02\ Ni^{+2}$	$+0.84\ Ni^{+2}$
Reactions	$+2.02\ Fe^{+3}$	$+0.16\ Fe^{+3}$
	$Ni_{0.98}Fe_{2.02}O_4$	$3\ Ni_{0.28}Fe_{2.72}O_{4.012}$

One notices immediately that, contrary to the situation in the Wagner hypothesis, the amounts of ions leaving one interface are not equal to those arriving and reacting at the other interface. This is because some of the ions leaving the interfaces are absorbed in altering the composition of the ferrite in the product layer and thus do not all arrive at the opposite interface available for formation of new product.

It also appears that additional Fe^{+3} must be supplied at the Fe_2O_3-ferrite interface to form ferrite of the required composition (based on the assumption that four molecules of Fe_2O_3 are consumed at that interface for four molecules of NiO consumed at the other interface). This merely illustrates that this reaction cannot be completely described in such simple terms; as we shall see later, NiO and Fe_2O_3 are not consumed at equal rates.

It is important to observe that nickel ferrite of composition differing greatly from the stoichiometric composition is formed at the opposite interfaces. At the NiO-ferrite interface the ratio of iron to nickel ions reacting to form ferrite is just slightly greater than two, while, at the Fe_2O_3-ferrite interface, the ratio becomes very large, approaching a value of ten for the case of a 1% O_2 atmosphere at 1200°C.

Since more iron ions must diffuse to the NiO-ferrite interface than nickel ions to the Fe_2O_3-ferrite interface in order to form ferrite product, it would appear that the product layer should develop much more rapidly in the direction of the Fe_2O_3 than toward the NiO. This implies that the original interface would lie much closer to the NiO than the Fe_2O_3. This picture is clouded by the observation of Sachs (29) that the nickel ions are less mobile in nickel ferrite than the iron ions. This effect would tend to move the original interface back toward the center of the reaction product. The combination of these two effects would result in the original interface being located somewhere in the center region of the ferrite product layer.

This conclusion is in agreement with the limited marker studies conducted. They showed that in all three atmospheres the original interface, as determined by the location of the marker, was in the center of the product layer, rather than closer to one or the other of the interfaces. Due to the relatively large particle size involved in the samples

relative to the thickness of the product layer, and the non-uniformity of product layer thickness, more accurate measurements of marker position within the product layer were not deemed justifiable.

Referring back to the disagreement found between measured and predicted cation concentrations in the diffusion couples, we have here another possible explanation for the discrepancy. It is obvious that the samples are not in the equilibrium state. The original premise was actually that the system was in a state which could be approximated by the assumption of steady state. It would then be possible to describe the system with relation to the equilibrium phase diagram. Even this does not seem to be an acceptable assumption.

A possible explanation is that the ferrite formed at the Fe_2O_3-ferrite interface is thermodynamically stable even though it has an iron-to-nickel ratio much greater than that predicted by the phase diagram. Since the nickel can diffuse through this high-ratio ferrite much faster than through the low-ratio ferrite, the ferrite formation at the Fe_2O_3-ferrite interface may be drawing nickel from the rest of the ferrite at a faster rate than it can be supplied by diffusion from the NiO-ferrite interface. Thus, the nickel concentration curves are lowered across the entire product layer. This would simultaneously cause an increase in the iron concentration curve.

Magnetic Moment Measurements

In analyzing the magnetic moment measurement as an indicator of degree of completion of the formation reaction, it is necessary to consider just what is being measured.

It has already been shown that the composition of the ferrite product is not constant, but varies across the entire distance between the reactants. On the basis of certain assumptions, it can be shown (see Appendix B) that the magnetic moment of nickel ferrite varies over a wide range, depending on the composition.

Thus, when we measure the magnetic moment per unit mass of a sample, we are actually measuring the magnetic moment of ferrite of constantly varying composition, and arriving at a result which corresponds to integration of the magnetic moment over the composition range.

More specifically, for nickel ferrite formed at 1200°C in a 100% O_2 atmosphere, the composition varies from 24.6 weight per cent nickel and 48.2 weight per cent iron at the NiO-ferrite boundary to 20.8 weight per cent nickel and 51.3 weight per cent iron at the Fe_2O_3-ferrite boundary. The magnetic moment of the ferrite formed varies from 2.042 Bohr magnetons at the former to 2.288 Bohr magnetons at the latter interface, a difference of 12 per cent. In a 1% O_2 atmosphere the composition varies from 24.6 weight per cent nickel and 48.2 weight per cent iron to 7.1 weight per cent nickel and 65.3 weight per cent iron at the opposite interfaces, while the magnetic moment varies from 2.042 to 3.43 Bohr magnetons,

a difference of 68 per cent.

The effect of magnetic moment variations on the samples prepared in different atmospheres is quite significant. In all cases the overall compositions in the ferrite layers tend toward a high iron-to-nickel ratio, as evidenced by the shapes of the concentration profiles. Thus, the magnetic moment of these samples will be heavily influenced by the preponderance of this high-ratio material. If we take the formation of the stoichiometric ferrite, $NiFe_2O_4$, with a magnetic moment of 2.0 Bohr magnetons, as a reference point for measurement of the amount of product formed, the magnetic moment measurements will indicate more ferrite than is actually present at any specific time. This in turn will indicate a faster rate of ferrite formation. Since this iron-to-nickel ratio effect on the magnetic moment is greater in the 1% O_2 samples than in the 100% O_2 samples, this effect will also indicate that the lower oxygen atmosphere increases the rate of nickel ferrite formation.

Thus far we have considered the case where there is both NiO and Fe_2O_3 existing in quantities sufficient to control the ferrite composition at both the NiO and Fe_2O_3 interfaces. We shall now consider what happens when one of the starting materials has been entirely consumed.

When one of the reactants is entirely consumed, the control it exerted on the ferrite composition due to equilibrium at that interface no longer exists. Thus the ferrite composition is now free to deviate from that

equilibrium composition.

Referring to the ternary phase diagram (Figure 3), we see that the ferrite product formed is always higher in iron content than the stoichiometric ferrite, $NiFe_2O_4$. Since the starting mixtures consisted of a one-to-one mole ratio of the reactants, it would be expected that the Fe_2O_3 is being consumed faster than the NiO. In addition, since the iron content is higher in the product of those samples reacted in lower oxygen atmospheres, it would be suspected that the Fe_2O_3 would be consumed faster in 1% O_2 than in the 100% O_2 atmosphere.

Analysis of Debye-Scherrer powder patterns of the samples reacted in 1% and 100% O_2 atmospheres for three hours at 1200°C showed that, while there was Fe_2O_3 present in the 100% O_2 sample, none was present in the 1% O_2 sample. Thus Fe_2O_3 is consumed faster in the samples reacted in the 1% O_2 atmosphere. It was not possible to compare rates of consumption of NiO and Fe_2O_3 using this method, since the diffraction lines for NiO and nickel ferrite fall close enough together that they cannot be separately identified in a study of this type.

Since the starting mixture consisted of a one-to-one mole ratio of the reactants, we know that the overall average composition should be that of $NiFe_2O_4$. We also know that this stoichiometric composition is unattainable under the conditions of atmosphere and temperature used in this

study. The phase diagram tells us that the final product, at equilibrium, should consist of nickel ferrite and (Ni,Fe)O, both compositions to be determined by the atmosphere under which equilibrium is achieved. Thus we know what the ultimate outcome of the reaction should be.

With (Ni,Fe)O existing at all times, this will determine the composition of the ferrite with which it is in contact. Since this ferrite composition is also that which the entire mixture should eventually reach, we can determine what must take place.

The iron concentration gradient will tend to level itself out by diffusing iron from those regions of high iron concentration to regions of lower iron concentration. However, when additional iron diffuses to the NiO-ferrite interface and raises the iron concentration of the ferrite, this additional iron reacts with (Ni,Fe)O to form more ferrite, thus maintaining the equilibrium ferrite composition.

As the composition throughout the entire ferrite portion of the sample tends toward the equilibrium composition at the NiO-ferrite interface, the lower iron-to-nickel ratio will result in a lower magnetic moment, and the apparent ferrite formation curve will decrease with time. As long as the magnetic moment contribution due to forming new product at the NiO-ferrite interface is greater than the decrease due to decreasing the iron-to-nickel ratio in the rest of the product layer, the magnetic moment curve will rise. The curve will reach a maximum when the two rates are equal, and

will begin to fall off when the decrease in magnetic moment due to falling iron-to-nickel ratio is greater than the increase due to new product formation.

The magnetic moment results in Figure 5 show that in those tests in which the reactants are present throughout the major portion of the reaction time, the reaction rate does appear to be significantly greater in 1% O_2 than in 100% O_2. This is in accord with the predicted results from both the cation transport and magnetic moment hypotheses.

It is possible to evaluate these effects independently by running the reaction at a lower temperature. Referring to Figure C-1, we see that below about 1000°C the effect of variations in the oxygen content of the atmosphere cause only a very small difference in the equilibrium composition of nickel ferrite at the Fe_2O_3-ferrite interface. Thus if we run the reaction at or below 1000°C, the effect of compositional differences on the magnetic moment measurement should be extremely small, and any differences in the rate of formation should be due primarily to effects of cation transport rates in the samples.

Figure 6, which shows the magnetic moment measurements following the formation of nickel ferrite in different atmospheres at 750°C, again shows that the atmospheres with low oxygen content result in a much faster reaction. Thus, we see that, although compositional variations can affect the apparent rates of formation, we are still able to conclude that the actual rate of formation is increased by decreasing

the oxygen content of the atmosphere.

The task of relating these magnetic measurements to the actual amount of product formed would be a rather formidable one, since one would have to know the amount of product as a function of composition present in the sample, and in turn determine its contribution to the overall magnetic moment.

The other possibility would be to prepare standard samples from different proportions of the ferrite and the starting components. Since the starting materials are consumed at unequal rates, this would have to be taken into account, and presumably a different set of standards would have to be prepared for each reaction atmosphere. Since the ferrite formed in the actual reaction varies in composition, this would also have to be taken into account when the standards are prepared. Unless these factors are considered when the standards are prepared, any comparisons made with them would have to be interpreted accordingly.

It is obvious from the earlier parts of this discussion that these problems must be taken into consideration for nickel ferrite formed at temperatures higher than about 1000°C, due to the variations in the product composition. Since the methods discussed in the Literature Survey for evaluating solid state reactions all depend on a knowledge of the volume of product formed, magnetic measurements on samples prepared above 1000°C are not suitable for these analyses.

If the reaction is conducted at a temperature well below 1000°C, where the effects on the magnetic moment due to compositional variations within the product are small, and where the differences in composition due to the different atmospheres is small, it should be possible to relate the magnetic moment measurements to volume of product formed. In this study artificial standards were prepared by mixing different amounts of $NiFe_2O_4$ with a one-to-one ratio of NiO and Fe_2O_3. In this manner it was possible to calibrate the Faraday balance to measure volume of product formed. With this information it is possible to evaluate the data obtained using the standard techniques. Figure D-1 shows the calibration chart for converting magnetic moments per unit mass to per cent of reaction completed for the samples prepared at 750°C.

Figures 7 and 8 show the results of the samples prepared at 750°C when analyzed using the Jander equation and the Ginstling-Brounshtein equation respectively. Since the basic assumption in both cases is that the reaction is controlled by cation diffusion through the product layer, and the data yield a straight line as predicted by both treatments, it is evident that the reaction being considered is actually diffusion-controlled.

Figure 9 shows the results of the magnetic moment measurements for extended periods of time. For these experiments the temperatures were selected so that the driving force due to overall cation concentration differences

were all about the same in the different atmospheres.

The curves of Figure 9 show that in general the theoretical analysis of the process appears to be correct, i.e., the curves reach a maximum value after which they decline gradually. We see that the curve for 1% O_2 at 1200°C reaches a maximum after about fourteen days, and the curve for 21% O_2 reaches a maximum after about one day. The position of the maximum cannot be determined for the 100% O_2 curve at 1450°C, but we do see that the maximum must be at considerably less than one day.

The data for 1350°C in 21% O_2 contain three points (22, 29 and 36 days) which are obviously not in agreement with the position in which the curve was drawn. Experimental difficulties during this series of tests permitted these samples to come into contact with the refractory in the furnace, and apparently the samples were contaminated to a considerable extent, thus affecting the magnetic moment measurements.

If we take the position of the maximum of the curves as an indication of the relative rates of reaction, and assume that the driving force due to the overall concentration gradient is the same in all three cases, we conclude that the increase in temperature causes a much faster reaction rate. It is also apparent that the rate of decrease of the curves is slow, indicating that homogenization is a relatively slow process in this system.

The results of this last set of experiments, which show

that the magnetic moment eventually decreases with time, support the theory that the reaction proceeds toward the same end product, regardless of the oxygen content of the atmosphere during the reaction, if sufficient reaction time is allowed. Thus we see that Figures 5 and 6 do not represent the complete reaction picture. This would seem to repudiate the conclusions of Okamura and Simoizaka (32) with respect to their "impurity" effect, which results in different end points for the reaction dependent on the "pressure of the outside air."

Lattice Parameter Measurements

Shafer's (4) work shows that there should be variations in the lattice parameter of the ferrite formed in these samples due to the variation in iron-to-nickel ratio throughout the product. Since any lattice parameter measurement would cover the entire range of compositions present, the only result available would be some sort of weighted average value. The overall composition of the ferrite is changing during the homogenization process, so some shift in this average lattice parameter should be occurring. Since the overall iron-to-nickel ratio is decreasing, the average lattice parameter would be expected to also decrease.

The results of Figures 10 to 12 show that, under all the experimental conditions employed, the average value of the lattice parameter does seem to decrease with reaction time. Although the actual calculated values show a definite lack of precision, the estimated standard deviations permit

the construction of a smooth curve which seems to be a reasonable representation of the data in each case.

In Figure 10, two of the data points are not in very good agreement with the curve drawn. The indicated allowable range for the nine-day value extends below the minimum allowable value (8.3394 Å for $NiFe_2O_4$), implying that perhaps the reported value is slightly low. No reason is known for the possible increase of the lattice parameter indicated by the 25-day sample.

Comparison of the diffraction patterns for the samples fired at 1300°C in 1% O_2 showed that the lines became sharper with increased firing time, agreeing with the results of Jefferson and Grimes (52).

Optimum Conditions for Reaction

We have seen that the apparent reaction rate can be affected by varying the composition of the atmosphere at any temperature, consequently producing a reaction product which varies with atmosphere composition, unless long times are allowed for homogenization. We have also seen that the apparent reaction rate can be increased by raising the reaction temperature while at the same time controlling the reaction product composition by controlling the atmosphere composition.

Let us now assume that the desired operation is one which results in a product of maximum uniformity in the shortest possible time. First we have seen that at any temperature, the product formed during the early stages has

a smaller composition range when it is fired in atmospheres of high oxygen content. Thus, for example, firing at 1200°C in 100% O_2 is desirable because the product varies in nickel content only from 24.6 to 20.8 weight per cent; however the reaction at this temperature is slow. If we decrease the oxygen content of the atmosphere, we increase the reaction rate, but we also form a product which varies widely in composition from one interface to the other. Since the homogenization process seems to be a very slow one, this situation is undesirable. Increasing the temperature of the reaction results in a faster reaction, but the resulting product is inherently less uniform, at least in the atmospheres used in this study.

In predicting the optimum conditions for performing the reaction, we employ the observation that increasing the oxygen pressure of the atmosphere results in a more uniform product. Since a high temperature, perhaps 1500°C or greater results in the desired fast reaction rate, it is apparent that oxygen pressures considerably in excess of one atmosphere will be necessary to give the desired uniformity of the product.

CONCLUSIONS

1. The optimum conditions for achieving a uniform nickel ferrite product from a mixture of NiO and Fe_2O_3 powders would be to fire the mixture at high temperatures (1500-1600°C), and conduct the reaction under a high oxygen partial pressure (considerably in excess of one atmosphere).
2. The rate of formation of nickel ferrite from NiO and Fe_2O_3 has been found to be controlled by the counter-diffusion of cations across the product layer.
3. Decreasing the oxygen partial pressure in the furnace atmosphere increases the actual rate of formation of nickel ferrite from NiO and Fe_2O_3.
4. Magnetic moment measurements can lead to ambiguous results in systems where the product formed is of non-uniform composition. It was established, however, that under proper experimental conditions the results obtained can be utilized in mathematically relating the data to an assumed reaction model.
5. Varying the oxygen content of the furnace atmosphere results in the formation of products of different compositions; however, if sufficient time is allowed for homogenization, the reaction will reach essentially the same end point, regardless of the furnace atmosphere.
6. The formation of the nickel ferrite product extends in both directions away from the original NiO-Fe_2O_3 interface,

as indicated by the inert marker studies conducted. No trends in the product formation direction due to the oxygen content of the furnace atmosphere were detected.

SUMMARY

This study was directed toward describing the reaction process during the formation of nickel ferrite from the component oxides, NiO and Fe_2O_3. Diffusion couple-type samples were prepared, fired under different oxygen partial pressures, and the resultant cation concentration profiles determined by the use of an electron microprobe. The corresponding oxygen contents were determined by relating the system to the ferrite region of the Fe-Ni-O phase diagram. In this manner the effect of variations in composition on the reaction process were predicted.

Magnetic moment measurements made on samples consisting of a one-to-one mole ratio of NiO and Fe_2O_3 powders intimately mixed, pressed into pellets, and fired in atmospheres of different oxygen contents for varying periods of time at 750°C and 1200°C indicated that the reaction rate is controlled by the counter-diffusion of cations across the ferrite layer. These measurements also led to the conclusion that a decrease in the oxygen content of the furnace atmosphere increases the rate of formation of nickel ferrite.

It was found that the magnetic moment measurement as an indicator of extent of reaction can yield ambiguous results in systems of this type, in which the product formed is of non-uniform composition. If the proper precautions are observed, the results can be related mathematically to an assumed reaction model to ascertain the validity of that model

in the situation under consideration. In this system, reaction temperatures of less than 1000°C yield a reaction product whose composition is uniform enough that the magnetic moment value is directly proportional to the amount of ferrite present.

It was determined that the optimum conditions for conducting this reaction are high reaction temperature (1500-1600°C) and high oxygen pressure (considerably in excess of one atmosphere). The high temperature is necessary to give a fast reaction. The high oxygen pressure reduces the composition variation in the product formed. Since the homogenization process is slow, it is desirable to form a uniform product and eliminate the necessity of long times for homogenization.

APPENDIX A

CALIBRATION OF ELECTRON MICROPROBE STANDARDS

Table A - 1

X-RAY FLUORESCENT ANALYSIS OF STANDARD FERRITES

Composition[1]	Ni-Bkgd[2]	Fe-Bkgd[2]	Ratio[3]	Area[4] Ni	Area[4] Fe	Ratio[5]
2.035	66.1	56.9	0.86	395	391	0.99
2.611	49.9	55.4	1.11	318	364	1.14
3.142	40.7	58.7	1.44	272	373	1.37
6.569	20.4	71.4	3.50	131.6	521	3.96
14.372	9.6	70.5	7.35	60.4	471	7.81
20%[6]	44.9	57.7	1.285	262	388	1.48
15%	30.4	59.5	1.96	197.5	387	1.96
10%	20.8	67.3	3.24	132	442	3.35
5%	11.2	78.4	7.00	72.8	540	7.42

1. Atomic ratio Fe:Ni
2. Peak height minus background
3. Ratio of peak heights
4. Area under diffractometer curve
5. Ratio of areas
6. Weight per cent nickel

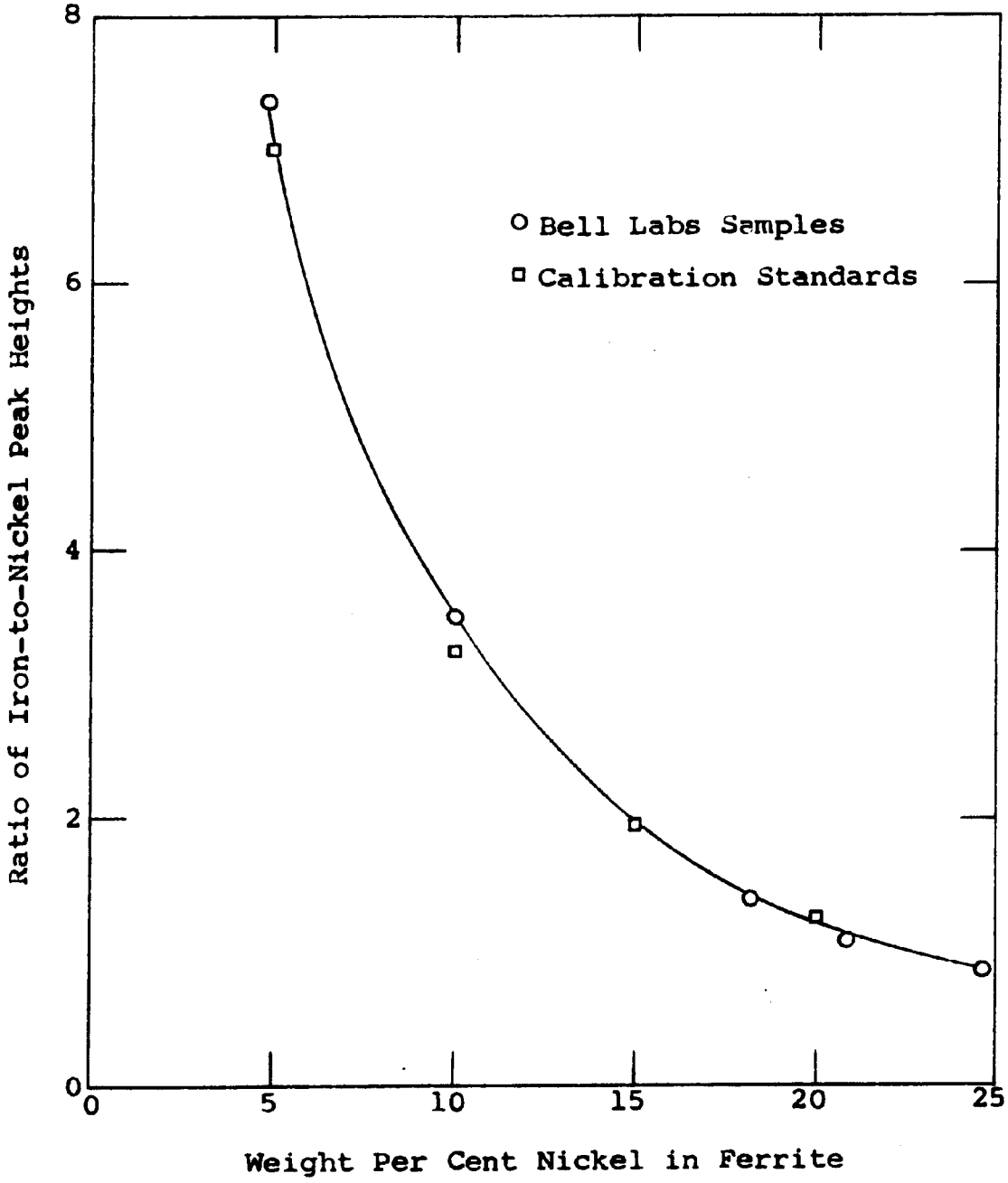


Figure A-1. Comparison by X-Ray Diffractometer Peak Height of Bell Labs Samples with Specially Prepared Standards

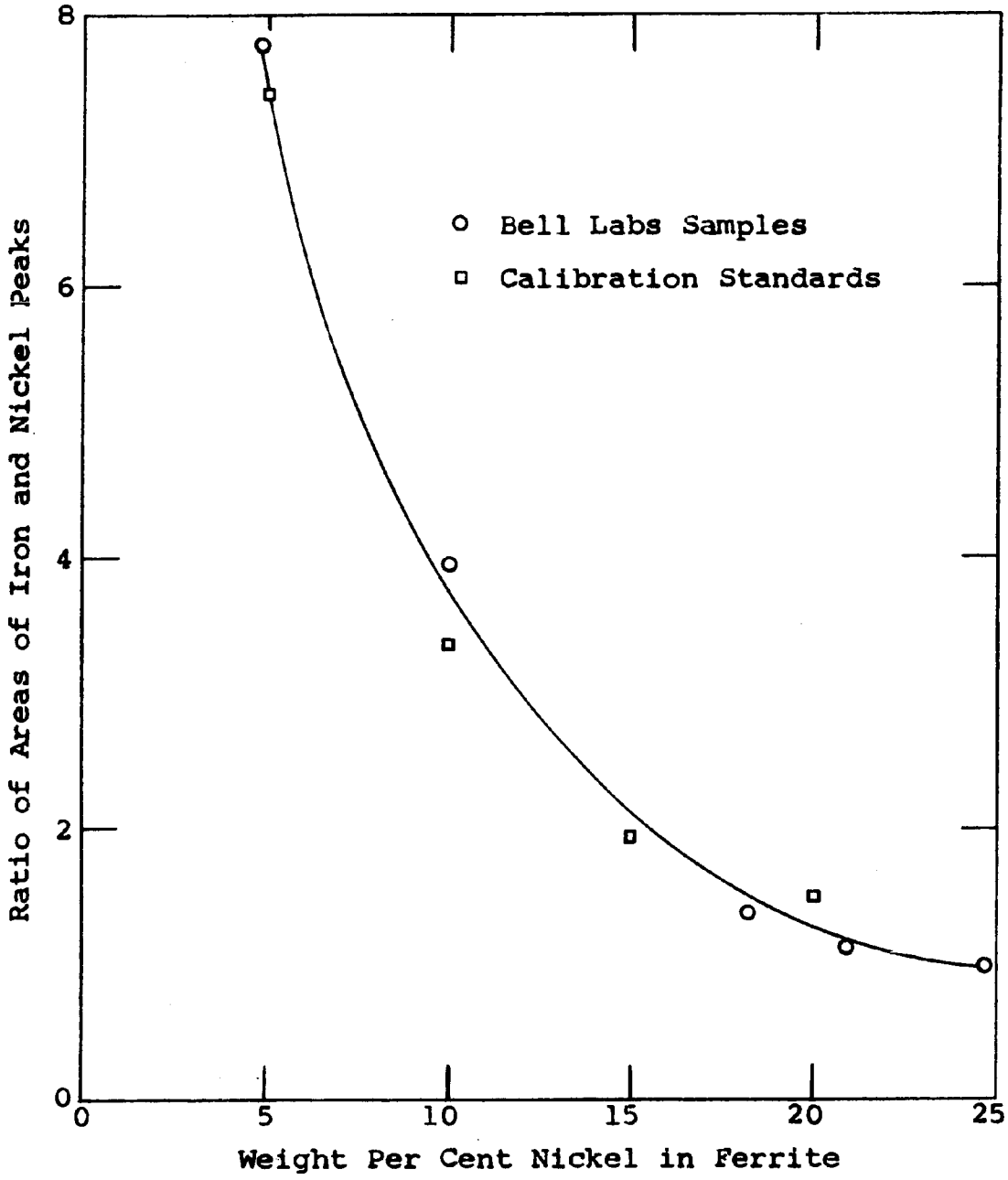


Figure A-2. Comparison by Area Under X-Ray Diffractometer Peaks of Bell Labs Samples with Specially Prepared Standards

APPENDIX B

MAGNETIC MOMENT OF NICKEL FERRITE

For the stoichiometric nickel ferrite, $NiFe_2O_4$, the magnetic moment, according to the Néel theory (48, 49), is visualized as follows:

A sites	B sites		Net Moment
Fe^{+3}	Ni^{+2}	Fe^{+2}	
←	→	→	
-5	+2	+5	$2\mu_B$

This assumes that the magnetic moment of an ion on an A site cancels the magnetic moment of a similar ion on a B site. The units are Bohr magnetons.

For the non-stoichiometric nickel ferrite, we must consider three different cases:

a. Fe:Ni < 2.0

b. Fe:Ni > 2.0, (Fe + Ni):O = 3:4

c. Fe:Ni > 2.0, (Fe + Ni):O < 3:4

The first case is not of interest at the present, since it occurs only under conditions of equilibrium with oxygen partial pressures in the atmosphere greater than one atmosphere.

The second case can be considered as follows: if we maintain the cation:anion ratio at 3:4, we must have all cation sites occupied. Thus, the iron which we add must replace Ni^{+2}, and must enter the structure in the form Fe^{+2}.

Schematically, we have:

A sites	B sites
Fe^{+3}	$(1 - x)Ni^{+2}$, $x\ Fe^{+2}$, Fe^{+3}

where x designates the number of Fe^{+2} ions which are substituted in place of Ni^{+2} ions per molecule of $NiFe_2O_4$. The magnetic moment calculation for this material will be considered below.

Now we consider the third case, where both the iron-to-nickel ratio and cation:anion ratio deviate from the stoichiometric composition. The additional feature in this form of the material is that when we disturb the cation:anion ratio, we disturb the ratio of available cation sites to occupied sites; i.e., by adding oxygen to the structure, we create additional cation vacancies which are not occupied by the cations present. From considerations of both material and charge balance, we have:

$$2y\ Fe^{+2} + \frac{y}{2}\ O_2 \longrightarrow 2y\ Fe^{+3} + y\ O^{-2} + \frac{3}{4}y\ \square_c$$

where $\square_c$ indicates a cation vacancy and y is the number of O^{-2} ions added to a $NiFe_2O_4$ molecule. If we assume that Ni^{+2} is not oxidized to Ni^{+3}, we see that we must have

$$0 \leq 2y \leq x$$

Now we shall look at the distribution of occupied cation sites. We know that essentially all the vacancies are located on the octahedral (B) sites. Thus, for y O^{-2} added to the ferrite molecule, we have:

	A sites	B sites			
Ion	Fe^{+3}	Fe^{+3}	Fe^{+2}	Ni^{+2}	$\square_c$
Quantity	$1 + a$	$1 + b$	$x - 2y$	$1 - x$	$\frac{3}{4}y$

where a and b represent adjustments in the Fe^{+3} ion positions due to the creation of cation vacancies. To determine a and b, we can say that the number of B sites is twice the number of A sites, leading to the expression:

$$2(1 + a) = 1 + b + x - 2y + 1 - x + \frac{3}{4}y$$

which reduces to

$$2a = b - \frac{5}{4}y.$$

But since we know that the additional Fe^{+3} must be equal to the Fe^{+2} which has been oxidized, we also have that:

$$a + b = 2y.$$

Solving these equations simultaneously, we find that

$$a = \frac{y}{4}$$

$$b = \frac{7}{4}y$$

and we have

	A sites	B sites			
Ion	Fe^{+3}	Fe^{+3}	Fe^{+2}	Ni^{+2}	$\square_c$
Quantity	$1 + \frac{y}{4}$	$1 + \frac{7}{4}y$	$x - 2y$	$1 - x$	$\frac{3}{4}y$
Moment	$\leftarrow$ -5	$\rightarrow$ $+2$	$\rightarrow$ $+4$	$\rightarrow$ $+5$	0

where the atomic moments have also been designated.

Now, for the overall magnetic moment of the sample, n_B we have:

$$n_B = \left[2(1 - x) + 4(x - 2y) + 5(1 + \tfrac{7}{4}y) - 5(1 + \tfrac{y}{4})\right]\mu_B$$

$$= (2 + 2x - \tfrac{y}{2})\mu_B.$$

Thus, we now have an expression relating the non-stoichiometric composition to the magnetic moment.

Sample Calculations

Basis: Calculated Phase Boundary Compositions

100% O_2 Atmosphere at 1200°C

Spinel - (Ni,Fe)O boundary

Ni = 0.14 Fe = 0.289 O = 0.571

$$\frac{Fe}{Ni} = K = \frac{0.289}{0.14} = 2.065$$

$$x = \frac{K-2}{K+1} = \frac{0.065}{3.065} = 0.021$$

$$Me = 0.14 + 0.289 = 0.429$$

$$O:Me = \frac{0.571}{0.429} = 1.331$$

$$3 \times 1.331 = 3.993 \simeq 4$$

$$\therefore y = 4 - 4 = 0$$

$$n_B = (2 + 2x - \tfrac{y}{2})\mu_B$$

$$= (2 + 2 \times 0.021)\mu_B = 2.042\mu_B$$

Spinel - Fe_2O_3 boundary

Ni = 0.118 Fe = 0.306 O = 0.576

$$K = \frac{Fe}{Ni} = \frac{0.306}{0.118} = 2.59$$

$$x = \frac{K-2}{K+1} = \frac{0.59}{3.59} = 0.164$$

$$Me = 0.118 + 0.306 = 0.424$$

$$O:Me = \frac{0.576}{0.424} = 1.36$$

$$3 \times 1.36 = 4.08$$

$$y = 4.08 - 4 = 0.08$$

$$n_B = (2 + 2x - \frac{Y}{4})\mu_B$$

$$= (2 + 2 \times 0.164 - 0.04)\mu_B$$

$$= (2 + 0.328 - 0.04)\mu_B = 2.288\mu_B$$

Difference

$$\frac{2.288 - 2.042}{2.042} \times 100 = \frac{0.246}{2.042} \times 100 = 12\%$$

1% O_2 Atmosphere at 1200°C

Spinel - Fe_2O_3 boundary

Ni = 0.14 Fe = 0.289 O = 0.571

Same as for 100% O_2

$$n_B = 2.042\mu_B$$

Spinel - Fe_2O_3 boundary

Ni = 0.04 Fe = 0.387 O = 0.573

$$K = \frac{Fe}{Ni} = \frac{0.387}{0.04} = 9.68$$

$$x = \frac{K-2}{K+1} = \frac{7.68}{10.68} = 0.72$$

$$Me = 0.04 + 0.387 = 0.427$$

$$O:Me = \frac{0.573}{0.427} = 1.34$$

$$3 \times 1.34 = 4.02$$

$$y = 4.02 - 4 = 0.02$$

$$n_B = (2 + 2 \times 0.72 - 0.01)\mu_B$$

$$= (2 + 1.44 - 0.01)\mu_B$$

$$= 3.43\mu_B$$

Difference

$$\frac{3.43 - 2.042}{2.042} \times 100 = \frac{1.388}{2.042} \times 100 = 68\%$$

APPENDIX C

SPINEL REGION OF Fe-Ni-O PHASE DIAGRAM

Table C - I

SPINEL FIELD BOUNDARY COMPOSITIONS AS A FUNCTION OF TEMPERATURE AND ATMOSPHERE[1]

% O_2 in atmos.	SPINEL - (Ni,Fe)O interface			SPINEL - Fe_2O_3 interface		
	Fe	Ni	O	Fe	Ni	O
			1000°C			
100	0.2883[2]	0.1403	0.5714	0.2897	0.1389	0.5714
21	0.2883	0.1403	0.5714	0.2919	0.1367	0.5714
1	0.2883	0.1403	0.5714	0.2936	0.1350	0.5714
			1100°C			
100	0.2883	0.1403	0.5714	0.2936	0.1350	0.5714
21	0.2883	0.1403	0.5714	0.3039	0.1245	0.5716
1	0.2883	0.1403	0.5714	0.3180	0.1100	0.5720
			1200°C			
100	0.2883	0.1403	0.5714	0.3063	0.1221	0.5716
21	0.2883	0.1403	0.5714	0.3246	0.1034	0.5720
1	0.2881	0.1405	0.5714	undetermined		
			1300°C			
100	undetermined			0.3481	0.0784	0.5736
21	0.2876	0.1410	0.5714			
1	0.2917	0.1369	0.5714	into Fe-O binary at ~1235°C		
			1400°C			
100	0.2828	0.1452	0.5714	0.3843	0.0410	0.5747
21	0.2938	0.1342	0.5714	into Fe-O binary at ~1390°C		
1	0.3056	0.1224	0.5714	in Fe-O binary		
			1500°C			
100	0.2899	0.1381	0.5714	into Fe-O binary at ~1465°C		
21	0.2982	0.1381	0.5714	in Fe-O binary		
1	0.3387	0.0893	0.5714	in Fe-O binary		
			1600°C			
100	0.2899	0.1381	0.5714	liquid		
21	0.3020	0.1260	0.5714	liquid		
1		liquid		liquid		

1. This table is based on the work of Darken and Gurry, Paladino, and Shafer
2. Contents expressed as atomic fractions

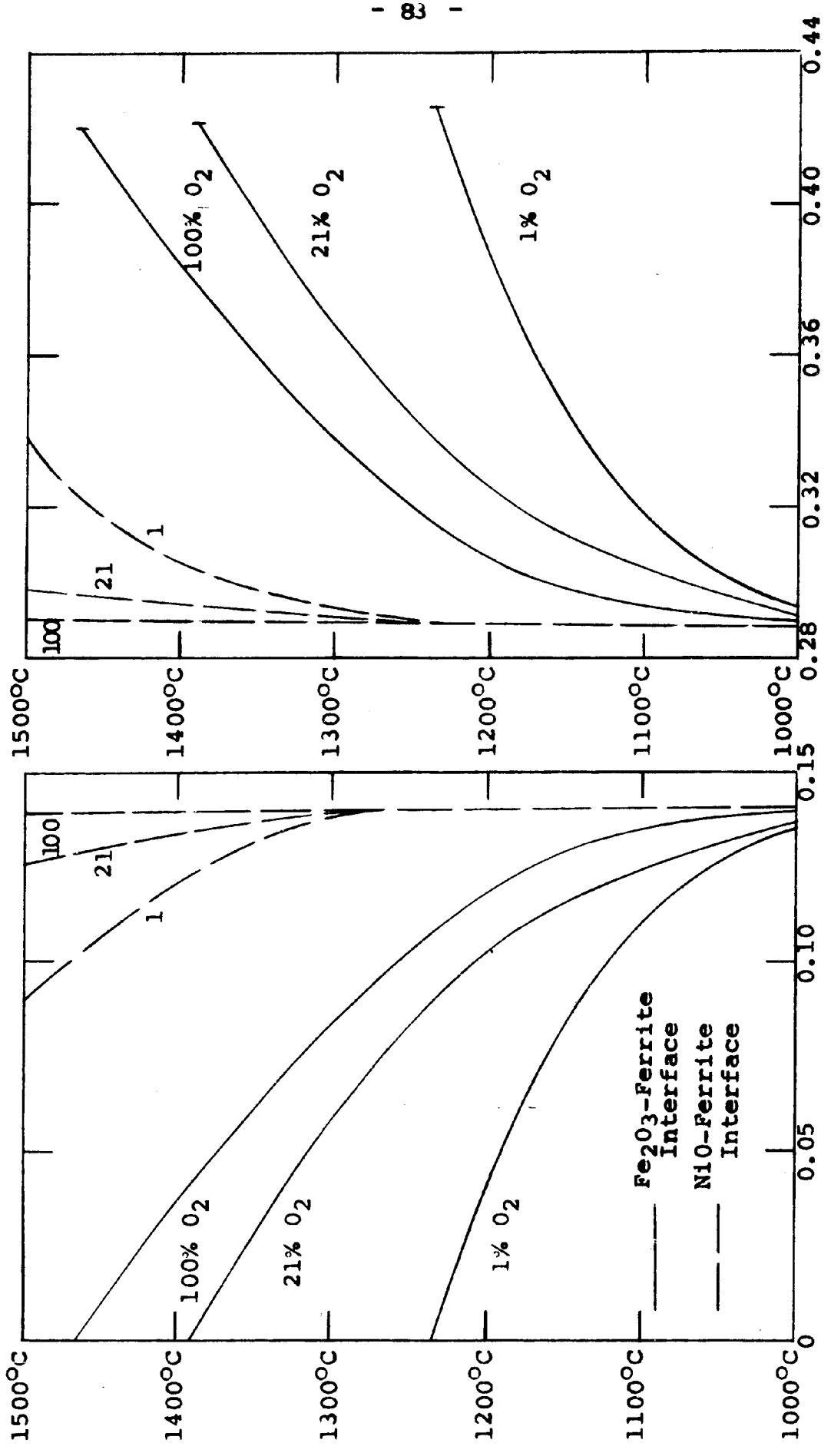


Figure C-1. Ferrite Compositions at NiO-Ferrite Interfaces and Fe_2O_3-Ferrite Interfaces as a Function of Furnace Atmosphere

Table C-II

Summary of Ferrite Compositions at Reactant-Product Interfaces in Nickel Ferrite System at 1200°C

Furnace Atmosphere		Spinel - (Ni,Fe)O atom frac	Spinel - (Ni,Fe)O wt per cent	Spinel - Fe_2O_3 atom frac	Spinel - Fe_2O_3 wt per cent
100% O_2					
	Ni	0.14	24.6	0.118	20.8
	Fe	0.289	48.2	0.306	51.3
	O	0.571	27.3	0.576	27.6
21% O_2					
	Ni	0.14	24.6	0.103	18.1
	Fe	0.289	48.2	0.325	54.4
	O	0.571	27.3	0.572	27.4
1% O_2					
	Ni	0.14	24.6	0.04	7.1
	Fe	0.289	48.2	0.387	65.3
	O	0.571	27.3	0.573	27.6

APPENDIX D

CALIBRATION OF FARADAY BALANCE

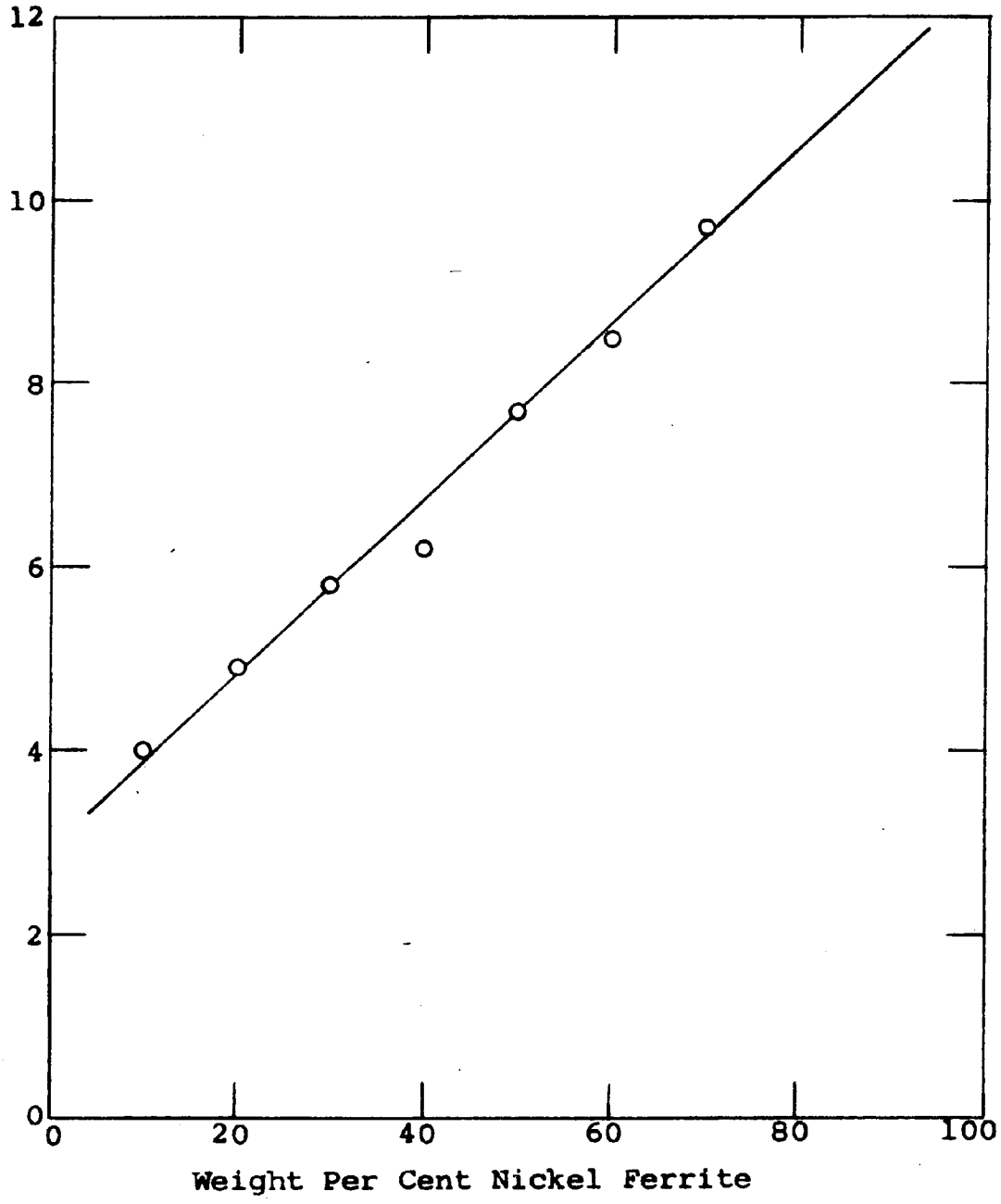


Figure D-1. Calibration Curve for Faraday Balance

BIBLIOGRAPHY

1. Wagner, C., "Über den Mechanismus der Bilding von Ionenverbindungen hoheren Ordnung (Doppelsalze, Spinelle, Silikate)," Z. phys. Chemie, B34, 309 (1936).

2. Wagner, C., "The Mechanism of the Movement of Ions and Electrons in Solids and The Interpretation of Reactions Between Solids," Trans. Faraday Society, 34, 851 (1938).

3. Skolnick, L. P., S. Kondo and L. R. Lavine, "An Improved X-Ray Method for Determining Cation Distribution in Ferrites," J. Appl. Phys., 29, 198 (1958).

4. Shafer, M. W., "Preparation and Properties of Ferrospinels Containing Ni^{+3}," J. Appl. Phys. Suppl., 33, 1210 (1964)

5. Gluck, J. V., "Precision Lattice Parameter Determination for a Cubic Material," Use of Computers in Metallurgical Engineering, The University of Michigan Engineering Summer Conferences, 1963, p. C-23.

6. Darken, L. S., and R. W. Gurry, "The System Iron-Oxygen. II. Equilibrium and Thermodynamics of Liquid Oxide and Other Phases," J. Am. Chem. Soc., 68, 798 (1946).

7. Paladino, A. E., "Phase Equilibria in the Ferrite Region of the System Fe-Ni-O," J. Am. Cer. Soc., 42, 168 (1959).

8. Shafer, M. W., "High Temperature Phase Relations in the Ferrite Region of the Fe-Ni-O System," J. Phys. Chem., 65, 2055 (1961).

9. Arkharov, V., A. Varskaya, M. Zvharavleva and G. Chufarov, "Reduction of Mixtures of Magnetic Iron Oxide with Nickel and Cobalt Oxides," Doklady Akad. Nauk. S.S.S.R., 37, 49 (1952)

10. Benard, J., Ann. Chim., 12, 5(1959).

11. Müller, S., and H. Schmalzried, "Fehlordnung in Kobaltferrit," Ber. der Bunsenges. für phys. Chemie, 68, 270 (1964).

12. Verwey, E. J. W., and P. W. Haayman, "Electronic Conductivity and Transition Point of Magnetite," Physica, 8 979 (1941).

13. Jefferson, C. F., "An Investigation of Reactions Involved in the Preparation of Ferrites," The University of Michigan, College of Engineering, Dept. of Electrical Engineering, Solid-State Devices Lab., Technical Report No. 7.

14. Jander, W., "Reaktionen im festen Zustande bei hoheren Temperaturen," Z. anorg. Chemie, 163, 1 (1927).

15. Carter, R. E., "Kinetic Model for Solid-State Reactions," J. Chem. Phys., 34, 2010 (1961).

16. Ginstling, A. M., and B. I. Brounshtein, "The Diffusion Kinetics of Reactions in Spherical Particles," J. Appl. Chem. (USSR), 23, 1249 (1950).

17. Carter, R. E., "Addendum: Kinetic Model for Solid-State Reactions," J. Chem. Phys., 35, 1137 (1961).

18. Turnbull, R. C., "Reinterpretation of the Reaction Kinetics of Nickel Ferrite," J. Appl. Phys., 32, 380 S (1961).

19. Lindner, R., "Some Problems in Solid State Chemistry," Dixieme Conseil de Chemie, 1956, p. 459.

20. Birchenall, C. E., "The Role of Spinel Oxides in the Oxidation of Iron and Its Alloys," Z. Elektrochemie, 63, 790, (1959).

21. Lindner, R., "Selbstdiffusion in Oxydsystemen," Z. Naturforsch, 10, 1027 (1955).

22. Condit, R., M. J. Brabers and C. E. Birchenall, "Self-Diffusion of Iron in Nickel Ferrite," Trans. AIME, 218, 768 (1960).

23. Himmel, L. E., R. F. Mehl and C. E. Birchenall, "Self Diffusion of Iron in Iron Oxides and the Wagner Theory of Oxidation," Trans. AIME, 197, 827 (1953).

24. Sun, R., "Diffusion of Cobalt and Chromium in Chromite Spinel," J. Chem. Physics, 28, 290 (1958).

25. Birchenall, C. E., "Mechanism of Diffusion in the Solid State," Metallurgical Reviews, 3, 225 (1958).

26. Romeijn, F. C., "Physical and Crystallographical Properties of Some Spinels," Philips Res. Rpts., 8, 304, 321 (1953).

27. McClure, D. S., "The Distribution of Transition Metal Cations in Spinels", Phys and Chem. Solids, 3, 311 (1957).

28. Schmalzried, H., "Die Selbstdiffusion von Fe in Magnetit in Zusammenhang mit der Elektron verteilung in Fe_3O_4 and Co_3O_4," Z. phys. Chem., NF31, 184 (1962).

29. Sachs, K., "Variations in the Structure across the Thickness of the Scale on Nickel Steels," J. Iron and Steel Inst., 185, 348 (1957)

30. Solymosi, F., and Z. G. Szabó, "The Effect of Defect Structure on the Rate of Spinel Formation," Magyar Kem. Foloirat, 67, 8 (1961), CA 55:14000d.

31. Beretka, J., and A. J. Marriage, "Determination of the Initial Formation Temperature of Nickel Ferrite Spinel," Nature, 203, 515 (1964).

32. Okamura, T., and J. Simoizaka, "The Reaction Kinetics of Spinel-Type Ferrite. I. Nickel Ferrite," Tohoku Univ. Res. Rpts., Sci., A2, 673 (1949).

33. Lindner, R., "Bildung von Spinellen und Silikaten durch Reaktion in festen Zustand, untersucht mit der Methode radioaktiver Indikatoren," Z. Elekt., 59, 967 (1955).

34. Carter, R. E., "Mechanism of Solid-State Reaction between Magnesium Oxide and Aluminum Oxide and between Magnesium Oxide and Ferric Oxide," J. Am. Cer. Soc., 44, 116 (1961).

35. Lindner, R., and Å. Åkerstrom, "Selbstdiffusion und Reaktion in Oxyd- und Spinellsystemen," Z. phys. Chem., NF6, 162 (1956).

36. Finch, G. I., and K. P. Sinha, "On Reaction in the Solid State," Proc. Royal Society, A239, 145 (1957).

37. _____, "An Electron-Diffraction Study of the Transformation α- Fe_2O_3 to γ- Fe_2O_3," Proc. Royal Society, A241, 1 (1957).

38. Sinha, K. P., Ph.D. Thesis, Univ. of Poona, Poona, India, 1956.

39. Tammann, G., "Über chemische Reaktionen in Gemengen fester Stoffe by erhohter Temperatur," Z. angew. Chemie, 39, 869 (1926).

40. Huttig, G. F., Handbuch der Katalyse, Springer-Verlag, Vienna, 1943, Vol. VI, p. 318.

41. Kedesdy, H., and G. Katz, "X-Ray Diffraction Study of the Formation of Some Ni-Zn Ferrites," Ceramic Age, 62, 29 (1953).

42. Forestier, H., "The Influence of Adsorbed Gases on the Reactivity of Solid Surfaces," Proc. Int'l Symp. on Reactivity of Solids, Gothenburg, 1952, p. 41.

43. Forestier, H., and J. P. Kiehl, "Influence de L'Adsorption Gazeuse sur la Vitesse de Reaction entre Oxydes Metalliques," J. Chim. Phys., 47, 165 (1950).

44. Henrich, G., "Uber den Einfluss der Gasatmosphare und des Pressdrucks auf Reaktionen in festen Zustand," Z. Elektrochemie, 58, 183 (1954).

45. Simon, A., and T. Schmidt, "Iron Hydrates and Iron Oxide," Z. Kolloidchemie, Erg.-Bd., 36, 77 (1925).

46. Kedesdy, H., and G. Katz, "X-Ray Diffraction Study of the Formation of Some Ni-Zn Ferrites," Ceramic Age, 62, 29 (1953).

47. Sakamoto, N., T. Asahi and S. Miyahara, "Magnetization of Magnesium Ferrite," J. Phys. Soc. Japan, 8, 677 (1953).

48. Néel, L., "Propriétés Magnétiques des Ferrites; Ferrimagnétisme et Antiferromagnétisme," Ann. Physiques, XII,3 137, (1948).

49. _____, "Saturation Magnetization of Certain Ferrites," Comptes Rend., 230, 190 (1950).

50. Epstein, D. J., and B. Frackiewicz, "Some Properties of Quenched Mg Ferrites," J. Appl. Phys., 29, 376 (1958).

51. Economos, G., "Solid Reactions in Ferrites," Kinetics of High Temperature Processes, W. D. Kingery, Editor, p. 243.

52. Jefferson, C. F., and D. M. Grimes, "A Study of the Preparation of Nickel-Zinc Ferrites," The University Of Michigan, College of Engineering, Dept. of Electrical Engineering, Solid-State Devices Lab., Technical Report No. 58.